J. Fluid Mech. (1990), *vol.* 218, *pp.* 299–335
Printed in Great Britain

The absorption of sound by perforated linings

By I. J. HUGHES[1] AND A. P. DOWLING[2]

[1] Topexpress Ltd, Poseidon House, Castle Park, Cambridge CB3 0RD, UK
[2] Department of Engineering, University of Cambridge, Cambridge CB2 1PZ, UK

(Received 6 February 1989 and in revised form 12 February 1990)

The efficiency of a perforated screen as a sound absorber can be greatly increased when a rigid surface is placed behind the screen, essentially because the sound can then interact many times with the perforations. We consider a practical application for a backed perforated screen with a bias flow through the perforations: the 'screech liner'. This is a perforated lining which is inserted in the afterburner section of jet engines to suppress the acoustically driven combustion instability commonly known as screech. A pressure drop across the screen ensures that a bias flow of cool air is produced; this flow protects the liner from the intense heat in the afterburner.

Our analysis was developed in answer to a clear need for a theory which can predict the optimal geometry and bias flow to produce a highly absorptive liner. We show that it is theoretically possible to absorb all the sound at a particular frequency. Experimental results are presented which show encouraging agreement with the theoretical predictions.

Screech is thought to be the excitation of a transverse resonant oscillation in the jet pipe, but the insertion of a liner inevitably changes the frequency of such resonances because the boundary condition at the wall is altered. We examine the effect of a liner on the resonances which occur in a cylinder and show that a well-designed liner may suppress resonances over a range of frequencies.

The effect of the hot axial jet flow on the performance of a liner has not previously received attention. A simple model to account for this flow is included in our analysis.

1. Introduction

In this paper we examine a practical application for sound-absorbent perforated screens where there is a bias flow through the screen.

In the 1940s, the quest for greater thrust from jet engines led to the introduction of afterburners. In these devices, fuel is injected upstream of a flame-stabilizing bluff body in the jet pipe. The reheat flame which is produced is a powerful source of sound, and it was soon discovered that a variety of acoustically driven combustion instabilities occurred. The two most common instabilities are referred to by the onomatopoeic terms 'buzz' and 'screech'. Buzz is the excitation of a longitudinal, 'organ pipe' resonance in the jet pipe. This instability has recently been studied in detail by Bloxsidge, Dowling & Langhorne (1988). Screech occurs at higher frequencies, when the flame excites a transverse mode of oscillation. Combustion instabilities are potentially hazardous, and there have been many attempts at suppressing them; Markstein (1964) reviewed much of the early work in this field. We are concerned here with screech only.

Research workers suspected that by inserting a sound-absorbent lining in the jet pipe, near the reheat flame, screeching combustion could be suppressed. The idea was

simply that if the sound produced by the flame at the screech frequency could be absorbed, then the sound level should remain acceptably low. The wall of the jet pipe was protected from the intense heat by a heat shield. This cylindrical lining has a pressure drop across it, and supplies cool air to the afterburner through a series of cooling rings. Experiments showed that an engine was less inclined to screech when additional holes were drilled in the heat shield. The mean pressure drop across the liner ensures that there is a bias flow. There is a need for a theory to determine the optimal combination of the perforation geometry and the bias flow.

Crude theoretical models have been developed in which the cylindrical lining was modelled as a plane collection of Helmholtz resonators without a bias flow; see, for example, Lewis & Garrison (1971). Each component 'cell' in such models is assumed to act independently, as if there were a honeycomb structure behind the perforated screen. In a real engine a honeycomb structure is impractical. Sound waves at oblique incidence must cause fluid to travel between the imaginary cells, and so these models are unrealistic.

Leppington & Levine (1973) presented a detailed theory for the reflection of sound by a plane rigid screen perforated with a regular array of circular or elliptical apertures and backed by a plane rigid wall. However, no mechanism by which sound energy could be absorbed was included. Their analysis shows that, unlike the simple Helmholtz resonator theory, the resonance frequency depends upon the angle at which sound is incident. For sound at normal incidence the resonance frequency coincides with the Helmholtz resonance frequency of an individual cell.

At typical screech frequencies, the wavelength of the sound is comparable with the radius of the jet pipe. The assumption that the lining may be treated as planar may therefore be unreliable. Also, the frequency at which screech may occur is commonly assumed to be unchanged by the insertion of a screech liner, but, since the boundary condition at the wall is changed, this is unlikely to be true.

Theoretical models of the mechanism by which sound energy is absorbed by perforates, such as those presented by Blackman (1960), Zinn (1970), Lewis & Garrison (1971), Melling (1973) and Cummings (1983, 1984), usually have no mean flow through the apertures. Without a mean flow, the absorption mechanism is complicated; above a certain sound level, around 100 dB, nonlinear viscous effects predominate (Ingard & Labate 1950).

The effect of blowing cooling air through a screech liner has received little attention. Some experimental work on the effects of a mean flow through the apertures in a small plane section of a typical screech liner was reported by Garrison *et al.* (1969). Bechert (1980) noted that a bank of Helmholtz resonators with a bias flow through the mouths was first proposed by Barthel (1958), and the idea that blowing air through a more elaborate liner could give adjustable absorption characteristics was investigated experimentally by Dean & Tester (1975). The interaction between sound and a steady low-Mach-number, high-Reynolds-number bias flow, such as the flow of cooling air, is of prime importance in determining the acoustic properties of perforates.

A more sophisticated theory is required. In this paper we describe work aimed at giving a clearer understanding of the acoustics of the type of perforated linings that may be used to suppress screeching combustion.

We shall examine the sound absorption properties of backed perforated screens with the aim of determining the role of the various parameters. When a plane backing plate is sufficiently far from the perforated screen for the local incompressible

flow in the mouths of the apertures to be unaffected by its presence, we can model the perforated screen as a homogeneous compliant plate. The rigid backing plate merely passively reflects the sound that is transmitted through the perforated screen. This scheme is also valid for a cylindrical liner under certain conditions which are discussed in the main text. We shall also examine the sound field produced by a source within a lined duct to see how the radiation from a source is affected by a perforated lining.

In a real jet pipe, there is an axial mean flow of hot gas which is separated from the liner by a slow moving layer of cool air. The effect of the hot mean flow on the acoustic properties of a sound-absorbent liner has not previously received attention. A simple model of this situation is presented in this paper. The cool layer is treated as a quiescent fluid except for the mean flow through the apertures. The variation in temperature and mean axial velocity is assumed to occur in a layer which is very thin in comparison to the wavelength of sound, and we treat the mixing layer as a discontinuity which separates the cool layer from the hot flow.

In §2 we develop a relatively general theory of the scattering of sound by a plane perforated screen in front of a backing plane. We then examine the absorptive properties of this arrangement when the perforations are circular apertures. An experiment to test this theory is described in §3. Armed with encouraging agreement between theory and experiment we move on to examine the effects of curvature on the absorptive properties of a liner in §4, and the sound field produced by a general source inside a lined cylinder in §4.1. An elementary extension of the theory to give an indication of the effects of a mean flow of hot gas along the duct is developed in §4.2. We conclude in §5 that the theory presented in this paper goes some way to improving our understanding of the acoustics involved in suppressing screech. We hope this work will be of use to design engineers.

2. The scattering of sound by a perforated screen with an infinite rigid backing plane

An infinite rigid wall occupies the plane $x_1 = -l$ of a Cartesian coordinate system (x_1, x_2, x_3). Parallel to this plane, at $x_1 = 0$, there is a thin rigid plate which contains a uniform, acoustically homogeneous, array of circular apertures of radius a. A steady bias flow of low Mach number and high Reynolds number is maintained outwards through the apertures. The geometrical arrangement is illustrated in figures 1 and 2.

We consider the reflection of plane waves of radian frequency ω by the backed screen. Since the perturbations of the compressible fluid are linear and inviscid, far from the screen on the scale of the apertures the pressure perturbation is to be a plane wave solution of the wave equation and may be written as

$$p = \mathrm{e}^{\mathrm{i}[k_2 x_2 + k_3 x_3 - \omega t]}[\mathrm{e}^{-\mathrm{i}k_1 x_1} + R\,\mathrm{e}^{\mathrm{i}k_1 x_1}], \tag{2.1}$$

where R is the reflection coefficient of the backed screen, and k_1, k_2, k_3 are the components of the wavenumber in the $1, 2, 3$ directions respectively. Between the perforated screen and the hard wall, the sound field may be written as

$$p = \mathrm{e}^{\mathrm{i}[k_2 x_2 + k_3 x_3 - \omega t]}[A\,\mathrm{e}^{-\mathrm{i}k_1 x_1} + B\,\mathrm{e}^{\mathrm{i}k_1 x_1}], \tag{2.2}$$

where A and B are complex constants.

Provided the aperture spacing is small in comparison with the wavelength and the

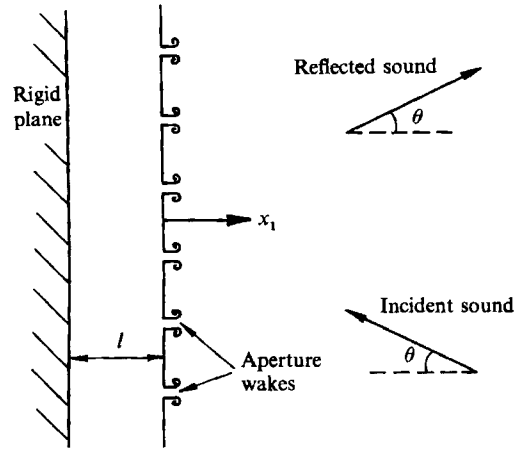

FIGURE 1. The geometry of the backed screen.

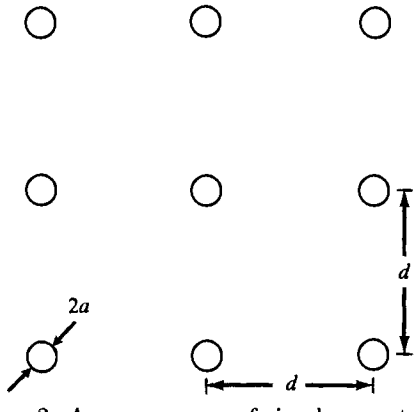

FIGURE 2. A square array of circular apertures.

cavity depth l greatly exceeds the aperture radius the acoustic properties of the screen can be described by the smoothed boundary condition

$$\frac{\partial p}{\partial x_1} = \eta[p]_{x_1=-0}^{x_1=+0} \quad \text{on} \quad x_1 = 0. \tag{2.3}$$

η, the effective compliance of the perforated screen, is simply related to the Rayleigh conductivity of an aperture. Howe (1979) determined the appropriate conductivity for circular apertures. In Howe's model an incident sound wave interacts with the mean bias flow to produce vorticity perturbations. The strength of the shed vorticity is determined from an application of the Kutta condition at the edge of an aperture. This vorticity initially convects away from the aperture with speed U, and ultimately decays into turbulence. For the square array of circles illustrated in figure 2, where the spacing between the apertures is d, we have the effective compliance

$$\eta = 2a\chi/d^2, \tag{2.4}$$

where χ is a function of the Strouhal number $\kappa a = \omega a/U$; we take U to be the mean velocity of the bias flow.

From Howe (1979)

$$\chi = \gamma - \mathrm{i}\delta, \tag{2.5}$$

where γ and δ are the real and positive functions

$$\gamma = \frac{I_1^2(\kappa a)\left[1+\frac{1}{\kappa a}\right]+\frac{4}{\pi^2}e^{2\kappa a}\cosh(\kappa a)K_1^2(\kappa a)\left[\cosh(\kappa a)-\frac{\sinh(\kappa a)}{\kappa a}\right]}{I_1^2(\kappa a)+\frac{4}{\pi^2}e^{2\kappa a}\cosh^2(\kappa a)K_1^2(\kappa a)};$$

$$\delta = \frac{\left[\frac{2}{\pi\kappa a}\right]I_1(\kappa a)K_1(\kappa a)e^{2\kappa a}}{I_1^2(\kappa a)+\frac{4}{\pi^2}e^{2\kappa a}\cosh^2(\kappa a)K_1^2(\kappa a)}.$$

$I_1(x)$ and $K_1(x)$ are modified Bessel functions.

The boundary conditions of vanishing normal velocity at $x_1 = -l$ and continuity of normal velocity at $x_1 = 0$, together with the linearized momentum equation, specify the sound field. We find that the reflection coefficient is given by

$$R = \frac{(ik_1/\eta)+1-(\mathrm{i}/\tan k_1 l)}{(ik_1/\eta)-1-(\mathrm{i}/\tan k_1 l)}. \tag{2.6}$$

This result is valid for any thin compliant plate, which can be described by equation (2.3), in front of a rigid backing plane.

The acoustic properties of the backed screen may also be described by the surface impedance Z which is defined to be the ratio of the surface pressure to the normal component of the surface velocity leading into the screen. This surface impedance is related to the reflection coefficient R through

$$Z = \left[\frac{1+R}{1-R}\right]\frac{\rho_0 c}{\cos\theta}, \tag{2.7}$$

where ρ_0 is the mean density, c the speed of sound and θ is the angle between the direction of propagation of the sound wave and the 1-axis.

We are particularly interested in the absorptive properties of these backed perforated screens. The absorption coefficient is simply related to the reflection coefficient R through

$$\mathcal{A} = 1-|R^2|, \tag{2.8}$$

because no sound is transmitted beyond the rigid plane.

On substituting the compliance η, given in (2.4), into (2.6), and rearranging the resulting expression, we obtain the reflection coefficient R for a plane backed screen with circular apertures, including the effects of vortex shedding:

$$R = \frac{(ik_0 d^2\cos\theta/2a\chi)+1-[\mathrm{i}/\tan(k_0 l\cos\theta)]}{(ik_0 d^2\cos\theta/2a\chi)-1-[\mathrm{i}/\tan(k_0 l\cos\theta)]}, \tag{2.9}$$

where $k_0 = \omega/c$ and $k_1 = k_0\cos\theta$. When there is no bias flow, $\chi = 1$. With the additional constraint $k_0 l\cos\theta \ll 1$, this expression reduces to that determined by Leppington & Levine (1973); the compactness condition was used in Appendix A of their paper. Leppington & Levine noted that the magnitude of their reflection coefficient is always unity: no sound energy is absorbed. With a bias flow through the holes, χ is complex. Then $|R| \leqslant 1$ and acoustic energy is absorbed. The absorbed energy appears as virtually incompressible vortical motions produced by the interaction of the sound and the mean flow at the rims of the apertures.

In elementary examinations of screech liners, where the backed screen is modelled as a bank of discrete Helmholtz resonators, it is assumed that a lining absorbs sound well at the Helmholtz resonance frequency. We can now examine the absorption characteristics of a lining more clearly.

Leppington & Levine pointed out that their backed screen reflects sound like a perfectly soft screen, that is, the reflection coefficient is -1, when the wavenumber $k_0 \cos\theta$ satisfies the resonance condition

$$k_0 \cos\theta = (2a/ld^2)^{\frac{1}{2}}. \tag{2.10}$$

Rayleigh (1899) showed that the resonance frequency of a Helmholtz resonator, which consists of an acoustically compact rigid container of volume V_0 in which there is an aperture with a Rayleigh conductivity K, is determined by the relationship

$$k_0 = (K/V_0)^{\frac{1}{2}}. \tag{2.11}$$

The Rayleigh conductivity of a circular aperture of radius a is $2a$ when there is no mean flow through the neck, and other dissipative mechanisms are ignored. The volume of each, imaginary, cell which makes up the backed screen is ld^2, and, for normally incident sound, $\cos\theta = 1$. Then the resonance condition for the backed screen is identical to the Helmholtz resonance condition, as expected. Equation (2.10) shows that the dependence of the resonance frequency on the angle of incidence of the sound takes a rather simple form. However, for large angles of incidence there is a significant difference between the resonance frequency predicted by assuming a cellular structure for the screen and that predicted by Leppington & Levine's theory.

In order to discuss our expression for the reflection coefficient, (2.9), which includes the effects of a mean flow through the apertures, it is useful to introduce a 'resonance parameter'

$$Q = (k_0 d \cos\theta)^2 l/2a, \tag{2.12}$$

proportional to the square of the frequency. Q is a convenient single-valued function of frequency which is unity at the modified Helmholtz resonance frequency given in (2.10). We can then rewrite (2.9) as

$$R = \frac{(Q/\chi) - \mathrm{i}k_0 l\cos\theta - [k_0 l\cos\theta/\tan(k_0 l\cos\theta)]}{(Q/\chi) + \mathrm{i}k_0 l\cos\theta - [k_0 l\cos\theta/\tan(k_0 l\cos\theta)]}. \tag{2.13}$$

This result shows that the reflection coefficient, and consequently the amount of sound energy absorbed by the screen, is a function of three non-dimensional variables: the resonance parameter Q, the Helmholtz number $k_0 l\cos\theta$, and the Strouhal number κa. One may expect from elementary Helmholtz resonator theory that the maximum sound absorption will occur near the modified Helmholtz resonance frequency, $Q = 1$. Any departure of the position of the maximum from $Q = 1$ arises as a consequence of the bias flow and cavity non-compactness.

The absorption coefficient $\mathcal{A} = 1 - |R|^2$ is plotted as a function of Q in figure 3(a) with the Strouhal number $\kappa a = 2$, and in figure 3(b) with the Helmholtz number $k_0 l\cos\theta = 0.5$. Perhaps the most striking feature of these plots is the efficiency of the backed screen as a sound absorber. For certain combinations of the dependent variables all the incident sound can be absorbed. However, the plots also show that designing a liner by merely choosing the resonance frequency, without consideration of the bias flow through the holes, does not guarantee a large absorption coefficient.

Figure 3 reveals that, for small values of the Helmholtz number $k_0 l\cos\theta$, the peak

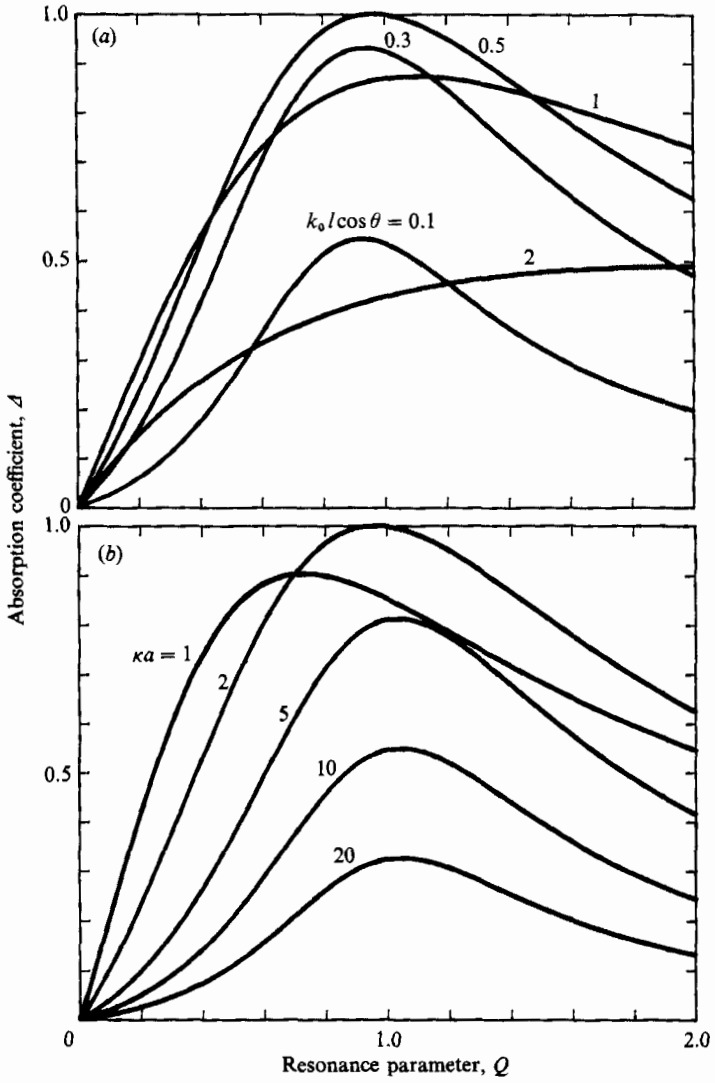

FIGURE 3. The absorption coefficient for a plane backed perforated screen with circular apertures as a function of the resonance parameter Q. (*a*) $\kappa a = 2$, (*b*) $k_0 l\cos\theta = 0.5$.

absorption, at a particular Strouhal number, occurs close to $Q = 1$. As the Helmholtz number is increased, so the resonance parameter becomes less useful as an indicator of the position at which the peak absorption will occur. We have already noted that the Helmholtz resonance theory relies on the cavity volume being acoustically compact. The relevance of the resonance parameter also decreases as the Strouhal number tends to zero, since the bias flow is then large, χ is significantly different from unity, and the resonance frequency shifts away from where $Q = 1$. If a sound-absorbent lining may be treated as planar, then the theory that we have presented in this paper may be used to design one that is highly absorptive.

In figure 4, the absorption coefficient has been plotted as a function of Strouhal number for different values of the cavity Helmholtz number $k_0 l\cos\theta$, *with the* resonance parameter set equal to unity. Such a family of curves should be useful when choosing the geometry and mean flow velocity for a particular absorptive

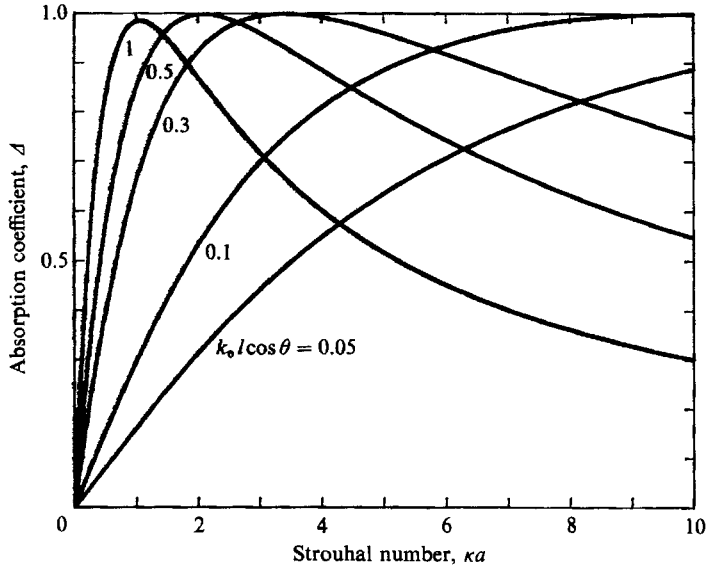

FIGURE 4. The absorption coefficient for a plane backed perforated screen when the resonance parameter Q is unity.

lining. For a given frequency, angle of incidence, and cavity depth, the parameter $k_0 l \cos\theta$ is fixed. The appropriate Strouhal number, and hence bias flow velocity, at which the absorption coefficient is sufficiently large can then be read from figure 4.

3. An experimental investigation of the acoustic properties of a plane backed perforated screen

In theory, a backed perforated screen can absorb all of the sound that is incident upon it at a particular frequency when there is a mean bias flow through the screen. In this section we present the results of the experimental investigation that we have carried out to test the theory. Garrison *et al.* (1969) did some experiments on the effect of a mean flow of air through a small plane section of a backed screen. However, that examination was limited to studying the way a mean flow could degrade the nonlinear absorptive properties of a liner. The absorptive properties of a screen in the presence of a bias flow of the type considered here has not previously been fully investigated experimentally.

We used the version of the popular 'impedance-tube' technique developed by Seybert & Ross (1977) to test the theory presented in §2. The experimental apparatus is illustrated schematically in figure 5. Two $\frac{1}{4}$ in. microphones, connected to a digital spectrum analyser, were mounted flush with the inner surface of a cylindrical brass tube of 95.6 mm nominal inside diameter. Backed screens were built up out of a thin perforated plate with circular apertures and a solid brass block which incorporated a cavity of the same inside diameter as the brass tube. There were four air inlets into the cavity through which a steady, but adjustable, flow of air was supplied. These were securely belted on to the end of the brass tube. Spacers could be introduced between the perforated plate and the end block so that the cavity depth could be adjusted. At the other end of the tube, loudspeakers were mounted and connected to a noise source. The distance to the microphone nearest to the sample was just over 0.3 m. This positioning was a compromise between being close

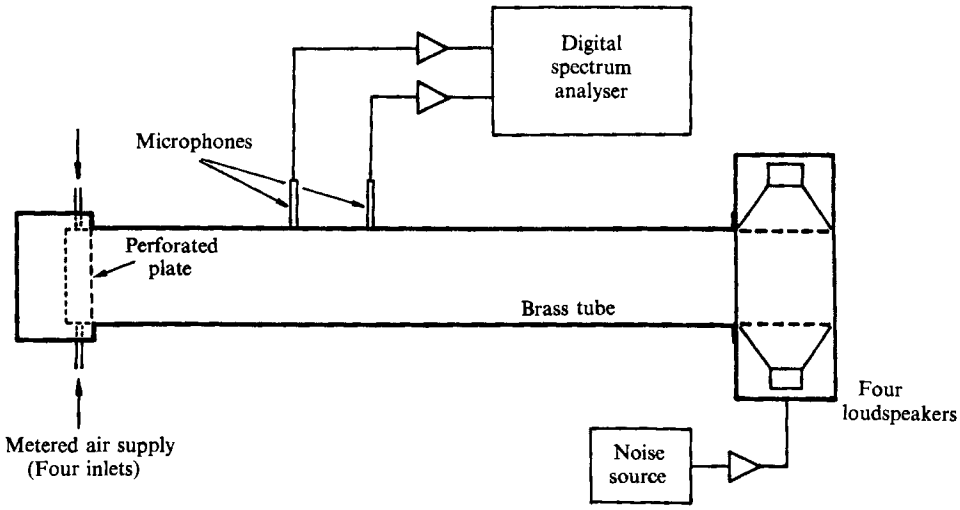

FIGURE 5. Schematic of the apparatus used for the experimental examination of the acoustic properties of a backed screen with circular apertures in the presence of a bias flow.

enough to minimize the propagation loss between the sample and the microphone, and far enough to avoid the near field effects. The spacing between the microphones, set equal to 91 mm, was also a compromise, mainly between placing the microphones far enough apart for the estimate of the effective separation to be well approximated by the distance between the microphone centrelines, and close enough for the frequency at which the spacing is equal to the half-wavelength to be sufficiently high. When the spacing is equal to the half-wavelength, the equations determined by Seybert & Ross which relate the measured quantities to the plane waves travelling to the left and right are ill-conditioned. We chose the spacing so that the frequency at which this occurred was just below the cut-on frequency where higher-order modes, as well as plane waves, propagate in the duct. Reliable measurements were then limited to frequencies below approximately 1.8 kHz.

Seybert & Ross showed that by measuring the auto- and cross-spectral densities at the two microphone positions when a sample is irradiated with white noise, in the frequency range appropriate for plane wave propagation, the acoustic properties of a simple impedance surface can be calculated. However, in the course of our theoretical analysis we neglected the linear contributions to the fluctuating flow in the apertures from the turbulence in the wake of the screen because they are of a different frequency to the incident harmonic sound. With white-noise excitation, this assumption is invalid. We therefore evaluated the response of the backed screen using discrete frequency excitation.

We first checked that the measured quantities were independent of the sound pressure level over the range 85 dB to 140 dB. The sound pressure level was not kept constant for the measurements and typically varied over this range. For each set of data, we varied either the frequency or the mean velocity through the apertures. From the measurements, we calculated the absorption coefficient Δ, the phase ϕ of the reflection coefficient, and the effective specific surface impedance $\hat{Z} = Z/\rho_0 c$. We found that the conditions could be varied over an interesting range using just two perforated plates, one with 24 apertures of radius 1.5 mm spaced 17 mm apart, which corresponds to an open-area ratio $\nu = 0.024$ based on the aperture spacing, and

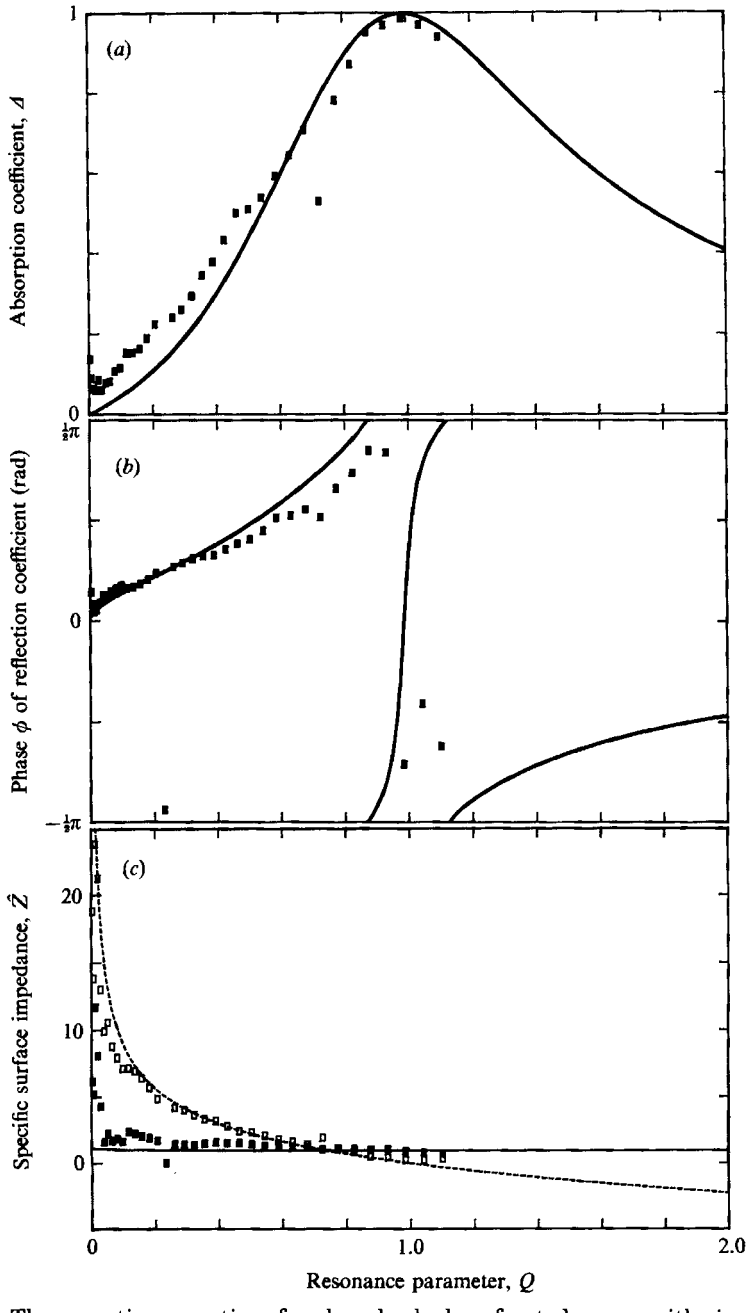

FIGURE 6. The acoustic properties of a plane backed perforated screen with circular apertures as a function of the resonance parameter Q when $M = 0.014$, $a/l = 0.15$, $al/d^2 = 0.052$. The solid lines, and the dotted line for $\mathrm{Im}(\tilde{Z})$, were produced using the theory presented in §2. Measured values: (*a*)–(*b*) filled squares, (*c*) filled squares for $\mathrm{Re}(\tilde{Z})$, open squares for $\mathrm{Im}(\tilde{Z})$.

another with 104, 1.5 mm radius apertures spaced 8 mm apart, corresponding to $\nu = 0.11$. The cavity depth was varied over the range 10–47.5 mm. The compactness condition $k_0 d \ll 1$ was satisfied since the maximum value for $k_0 d$ was 0.56.

In §2 we showed that only three non-dimensional variables are necessary to

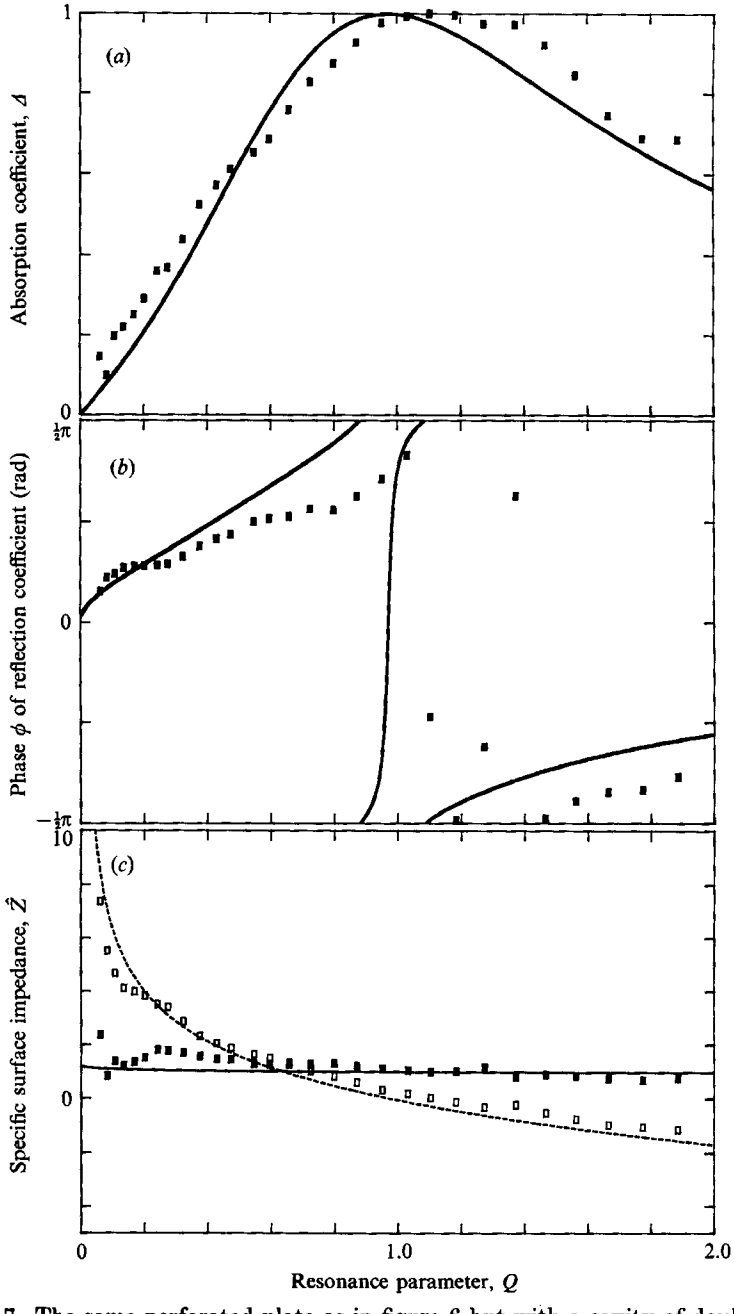

FIGURE 7. The same perforated plate as in figure 6 but with a cavity of double the depth: $a/l = 0.075$, $al/d^2 = 0.1024$.

describe the acoustic properties. However, those variables are all frequency dependent. It is thus convenient to present the experimental results using the following four non-dimensional parameters: the resonance parameter Q, which was introduced in §2 and is equal to $k_0^2 ld^2/2a$ for normally incident sound, the Mach number M, based on the mean flow velocity in the mouths of the apertures, and two parameters, al/d^2 and a/l, which depend upon the geometry alone. The Mach

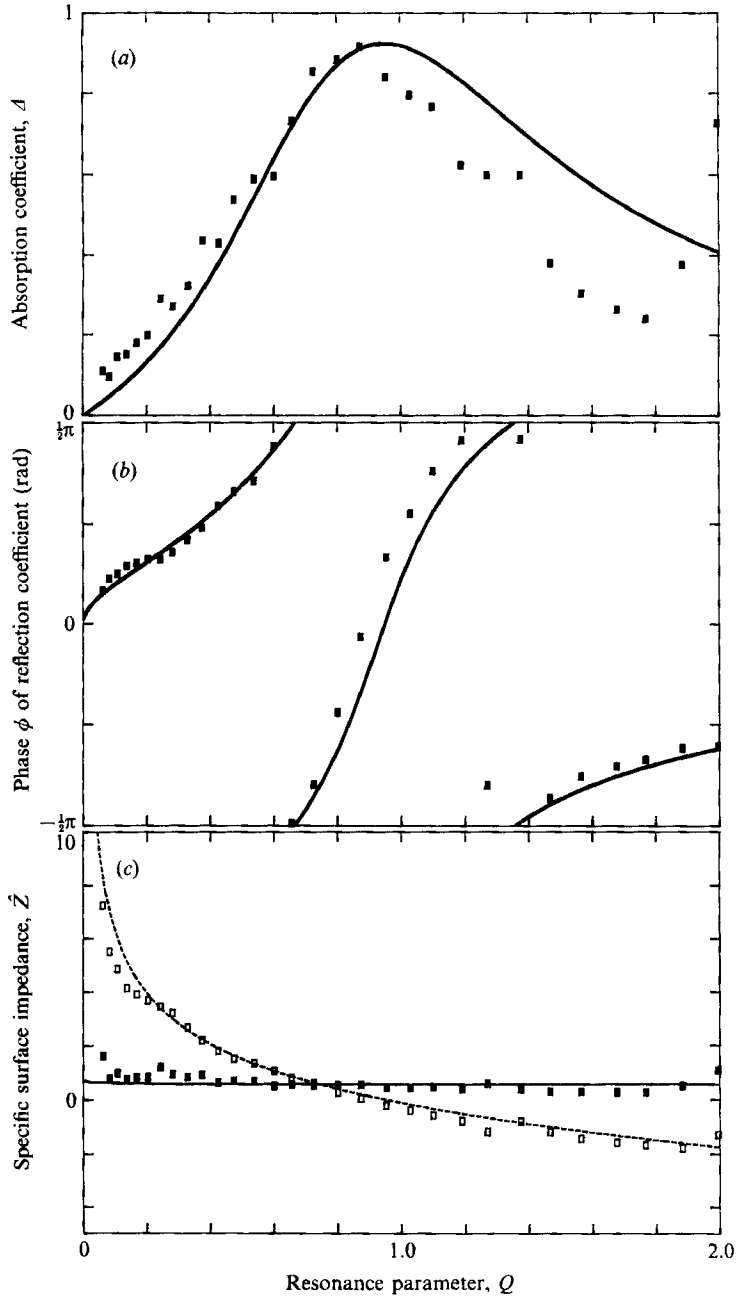

FIGURE 8. The same geometry as in figure 7 but with a different bias flow; $M = 0.086$.

number, $M = U/c$, is therefore simply related to the Strouhal number $\kappa a = \omega a/U$. In terms of the new parameters, the Strouhal number is given by

$$\kappa a = [2Q(al/d^2)]^{\frac{1}{2}}(a/l)M. \tag{3.1}$$

A representative set of experimental results is presented in figures 6–12. The theoretical properties are plotted for comparison. We have used equations (2.9) and (2.5) for the reflection coefficient, (2.8) for the absorption coefficient, and (2.7),

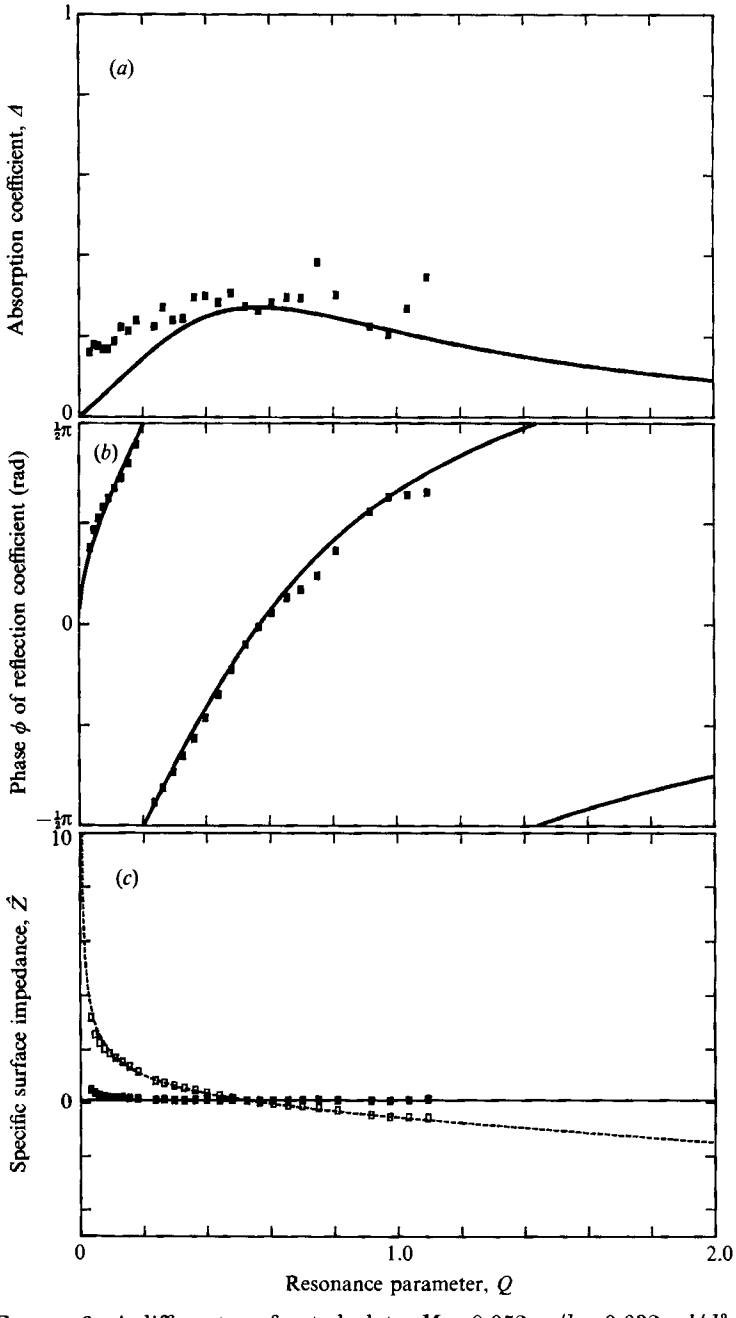

FIGURE 9. A different perforated plate. $M = 0.052$, $a/l = 0.032$, $al/d^2 = 1.06$.

divided by $\rho_0 c$, for the specific surface impedance. These results were obtained using the plate with 24 apertures, except for figure 9. The agreement between the theoretical and experimental acoustic properties is very encouraging. In figures 6–9, Δ, ϕ, and $\hat{Z}$, are plotted as a function of the resonance parameter. We see from figure 7 that the theoretical prediction of total sound absorption, at a particular frequency, can be attained in practice. When the parameters are altered to produce a less efficient sound absorber, the correlation between the theory and experiment is also

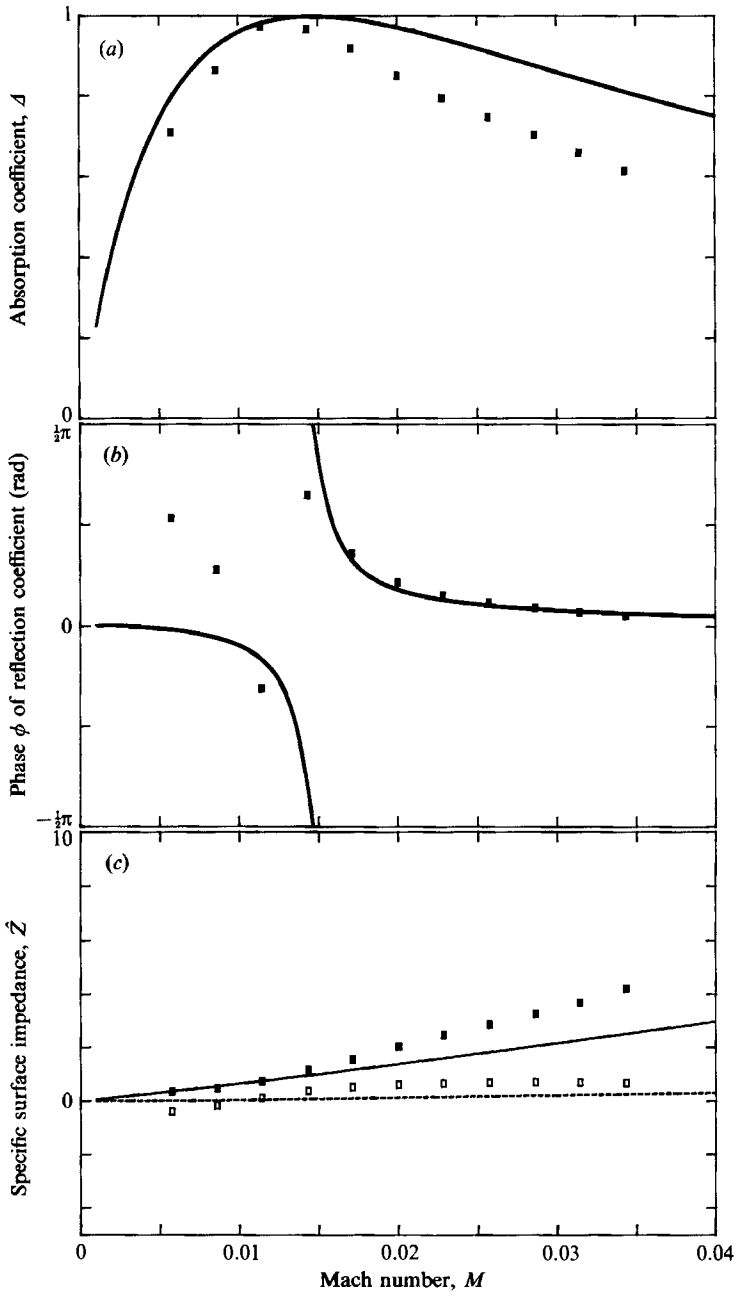

FIGURE 10. The acoustic properties of a plane backed perforated screen with circular apertures as a function of the Mach number M when $a/l = 0.075$, $al/d^2 = 0.1024$, $Q = 1$. The solid lines, and the dotted line for $\mathrm{Im}(\hat{Z})$, were produced using the theory presented in §2. Measured values: (*a*)–(*b*) filled squares, (*c*) filled squares for $\mathrm{Re}(\hat{Z})$, open squares for $\mathrm{Im}(\hat{Z})$.

rather good, as figures 8 and 9 reveal. In figures 10–12 the comparison between experiment and theory is shown as a function of the Mach number M. Here the agreement is also notable, but the variation of the real part of the surface impedance, which is responsible for the energy absorption, appears to be less reliably predicted than the imaginary part.

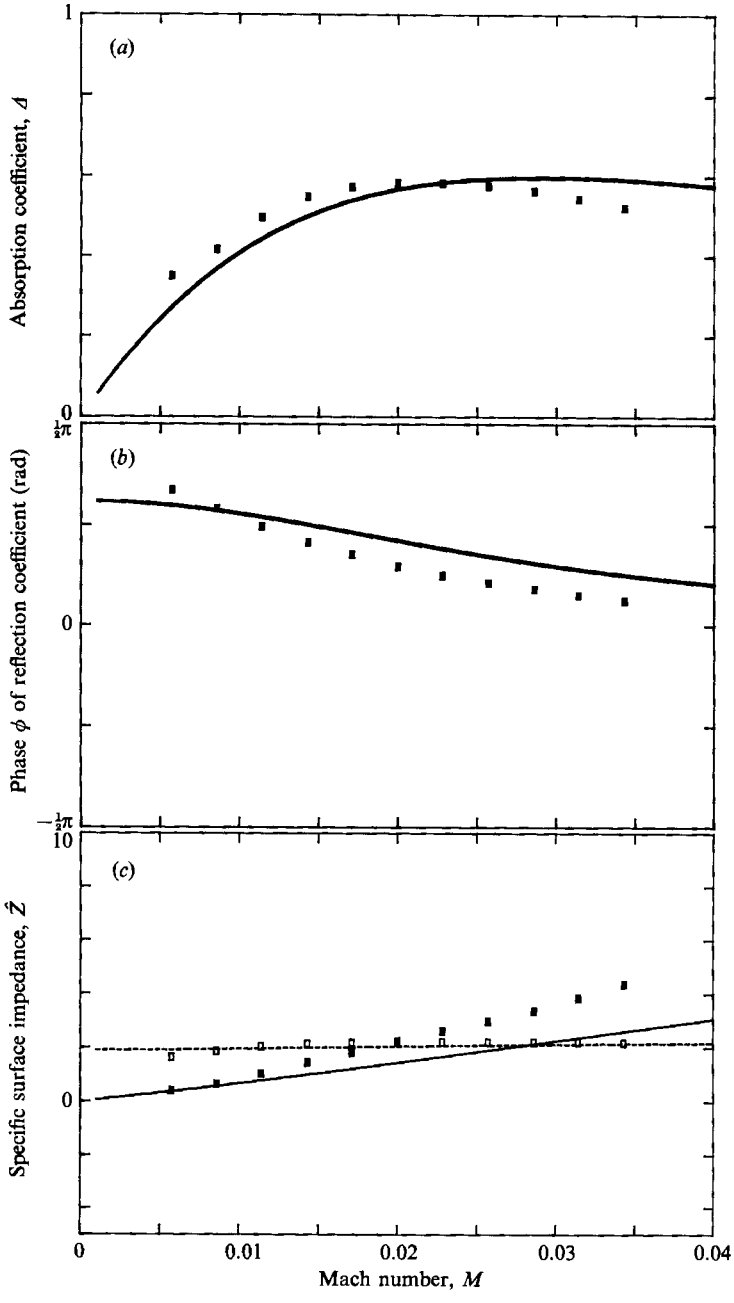

FIGURE 11. The same geometry as figure 10 but at a different frequency so that the resonance parameter $Q = 0.043$.

There is much scope for error in the experimental results. We have already mentioned the sensitivity to error which arises when the microphone spacing is nearly equal to the half-wavelength of the sound. This accounts for scatter in the results at the upper end of the range of Q in figures 6–9. Seybert & Ross also pointed out that errors are magnified when the phase ϕ of the reflection coefficient is small and this accounts for much of the scatter in the results presented here, particularly

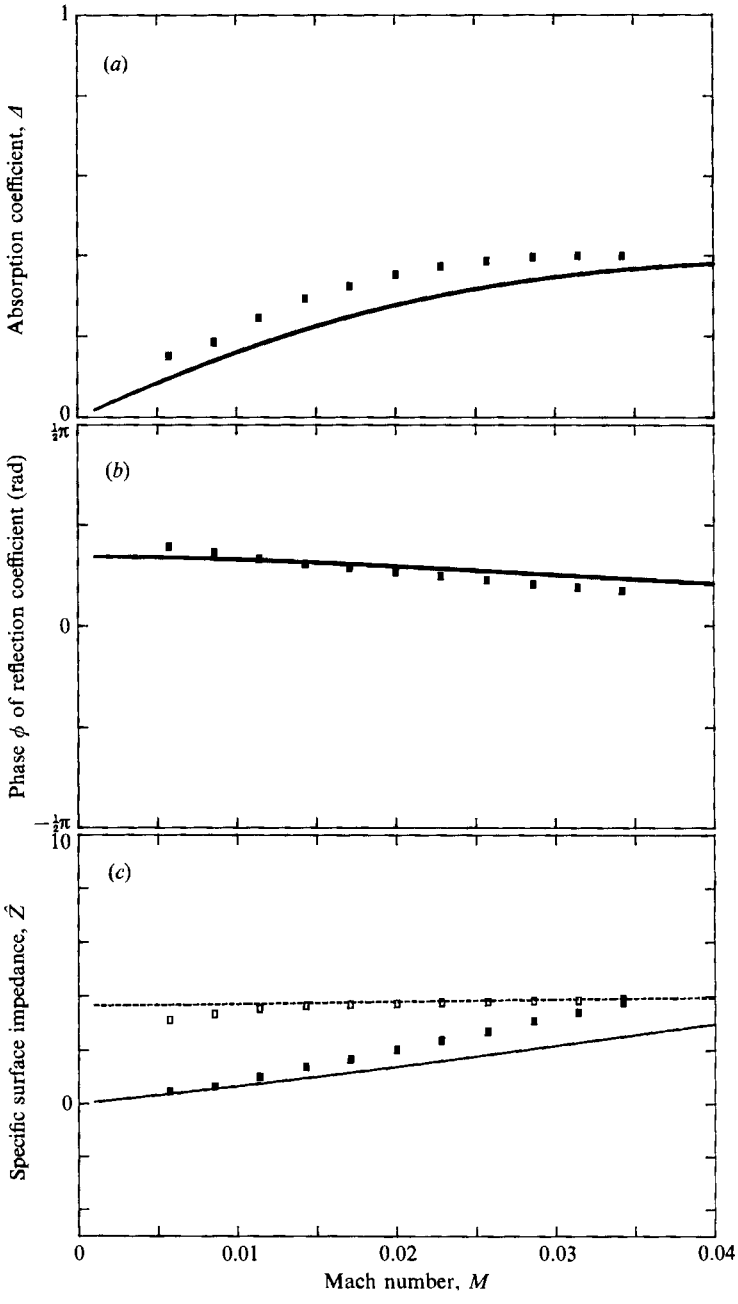

FIGURE 12. The same perforated plate as in figure 10 except but with a cavity of half the depth and at a different frequency. $a/l = 0.15$, $al/d^2 = 0.052$, $Q = 0.33$.

in figure 10. Other sources of error include the non-uniformities in the perforated plates, the fact that the plates have a finite thickness, and problems associated with the method of providing a steady mean flow through the apertures. Seybert & Soenarko (1981) and Bodén & Abom (1986) discuss other sources of error inherent in the experimental method. However, we content ourselves with the indication that

the theory presented in this paper predicts the acoustic properties of a plane backed perforated screen rather well despite these sources of error.

4. The scattering of sound inside a cylinder lined with a perforated sheet

A screech liner is cylindrical. In this section we examine the effects of curvature on the absorptive properties of a perforated lining. We consider the geometry depicted in figure 13. A rigid cylinder of unlimited length is lined with a thin, but rigid, perforated sheet. The perforations are an acoustically compact distribution of small circular apertures and a mean flow, of the type already considered, is directed radially inwards; further limitations on the size of the apertures are discussed later. A cylindrical polar coordinate system (r, ϕ, z) is centred on the axis of this lined cylinder.

Screech is thought to be the excitation of a transverse acoustic resonance in a duct. These resonances are associated with standing wave patterns which arise as a consequence of constructive interference between travelling waves; the wavelength is of the same order of magnitude as the duct radius. We wish to examine the effectiveness of a perforated lining in suppressing screeching combustion. We shall consider the sound field to consist of a linear combination of Hankel functions, H_n. All components of the sound field are then proportional to $\exp[-\mathrm{i}(\omega t - k_z z - n\phi)]$, where k_z is the wavenumber in the z-direction. This factor is suppressed in the following analysis.

We have already mentioned that the compliance of a perforated screen is simply related to the Rayleigh conductivity of a single aperture in a rigid baffle. The relationship between these quantities is derived by smearing the perturbation velocity distribution over the surface to give a continuous velocity distribution. This procedure is valid because the sound is insensitive to the local detail on the surface. If the perforated lining is approximately plane within a distance from the aperture that is large in proportion to the aperture dimension, then the Rayleigh conductivity, and hence the compliance, should be insignificantly affected by the curvature, Rayleigh (1945, §306), in his discussion of the concept of an aperture's conductivity, noted that this constraint on the use of the conductivity should be sufficient.

In our cylindrical coordinate system the compliance relationship is

$$\frac{\partial p}{\partial r} = \eta [p]_{r=r_1-0}^{r=r_1+0} \quad \text{on} \quad r = r_1. \tag{4.1}$$

We shall find it useful to introduce a reflection coefficient R for this lined infinite cylinder since this is simply related to the absorption coefficient Δ through

$$\Delta = 1 - |R|^2. \tag{4.2}$$

The sound pressure p in the region $r_0 < r \leqslant r_1$, which is exterior to the region containing a source of sound ($r \leqslant r_0$), may then be written in the form

$$p = A[H_n^{(1)}(\gamma r) + RH_n^{(2)}(\gamma r)], \tag{4.3}$$

where $\gamma = (k_0^2 - k_z^2)^{\frac{1}{2}}$ and A is a constant. At this stage we are not concerned with what happens in the source region. In the cavity between the perforated lining and the rigid cylinder, $r_1 \leqslant r \leqslant r_2$,

$$p = BH_n^{(1)}(\gamma r) + CH_n^{(2)}(\gamma r), \tag{4.4}$$

where B and C are constants. The constants A, B and C in (4.3) and (4.4) are

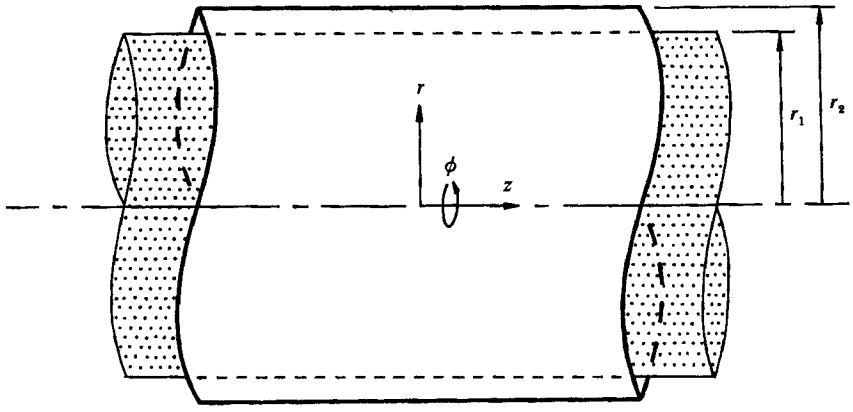

FIGURE 13. The geometry of the lined cylinder.

eliminated by applying the boundary conditions of vanishing normal velocity at $r = r_2$, the compliance relationship (4.1), and continuity of normal velocity at $r = r_1$; the latter condition is implicit in the compliance relationship.

We then find that, in terms of the compliance η,

$$R = \frac{\eta\beta[H_n^{(1)}(\gamma r_1) - \alpha H_n^{(2)}(\gamma r_1)] - \gamma(\alpha-\beta) H_n^{(1)'}(\gamma r_1)}{\eta[\alpha H_n^{(2)}(\gamma r_1) - H_n^{(1)}(\gamma r_1)] + \gamma(\alpha-\beta) H_n^{(2)'}(\gamma r_1)}, \tag{4.5}$$

where the prime denotes differentiation with respect to the argument and we have introduced the following shorthand notation:

$$\alpha = \frac{H_n^{(1)'}(\gamma r_1)}{H_n^{(2)'}(\gamma r_1)}, \quad \beta = \frac{H_n^{(1)'}(\gamma r_2)}{H_n^{(2)'}(\gamma r_2)}. \tag{4.6}$$

As with the plane liner, the acoustic properties of the lined cylinder may be described by the surface impedance Z, which for this geometry is given by

$$p = \frac{Z}{i\omega\rho_0}\frac{\partial p}{\partial r} \quad \text{on} \quad r = r_1. \tag{4.7}$$

We find that this impedance is related to the reflection coefficient by the expression

$$Z = \frac{i\omega\rho_0}{\gamma}\left[\frac{H_n^{(1)}(\gamma r_1) + R H_n^{(2)}(\gamma r_1)}{H_n^{(1)'}(\gamma r_1) + R H_n^{(2)'}(\gamma r_1)}\right]. \tag{4.8}$$

When the radius of the perforated lining becomes large in comparison with the wavelength, we expect the reflection coefficient in (4.5) to bear a simple relationship to the plane wave reflection coefficient presented in §2. On replacing the Hankel functions in (4.5) by their asymptotic forms, we find that as $\gamma r_1 \to \infty$

$$R \sim \exp[2i(\gamma r_1 - \tfrac{1}{2}n\pi - \tfrac{1}{4}\pi)]\frac{[i\gamma/\eta + 1 - i/\tan\gamma l]}{[i\gamma/\eta - 1 - i/\tan\gamma l]}, \tag{4.9}$$

where here $l = r_2 - r_1$. The radial wavenumber, γ, is equivalent to the wavenumber k_1 which appears in the expression (2.6) for the reflection coefficient of a plane backed screen, and we see that these results only differ by the exponential function which premultiplies equation (4.9). This function affects only the phase of R, and appears

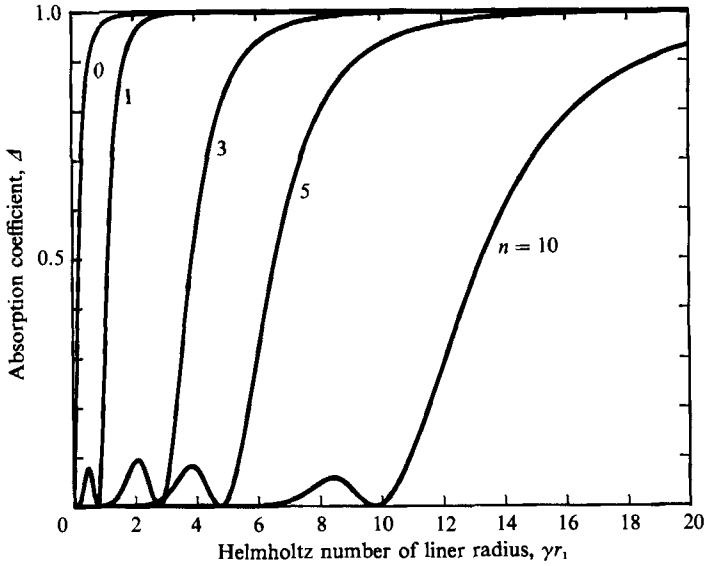

FIGURE 14. The absorption coefficient for a cylindrical liner within a rigid cylinder expressed as a function of the Helmholtz number γr_1 when $Q = 1$, $\kappa a = 2$, $\gamma l = 0.5$. The curves are for sound fields with different azimuthal variation.

because the definition of the reflection coefficient in (4.3) is slightly different from that in (2.1).

Before moving on to examine the absorptive properties of a cylindrical perforated lining we note that (4.5) can be rearranged into a form where the Wronskian

$$H_n^{(1)}(\gamma r_1) H_n^{(2)'}(\gamma r_1) - H_n^{(2)}(\gamma r_1) H_n^{(1)'}(\gamma r_1) = -4\mathrm{i}/\pi\gamma r_1 \tag{4.10}$$

(Abramowitz & Stegun 1965) appears. We then obtain an alternative form for the reflection coefficient:

$$R = -\alpha \frac{[4\mathrm{i}\beta l/\{\pi r_1(\alpha-\beta) H_n^{(1)'}(\gamma r_1) H_n^{(2)'}(\gamma r_1)\} + \gamma^2 l/\eta]}{4\mathrm{i}l/\{\pi r_1(\alpha-\beta)[H_n^{(2)'}(\gamma r_1)]^2\} + \gamma^2 l/\eta}. \tag{4.11}$$

The effective compliance η of a screen with circular apertures, through which a steady mean flow is forced, was given in (2.4) and (2.5). On substituting this compliance for η in equation (4.11) we obtain the reflection coefficient R for a cylindrical liner with circular apertures:

$$R = -\alpha \frac{[4\mathrm{i}\beta l/\{\pi r_1(\alpha-\beta) H_n^{(1)'}(\gamma r_1) H_n^{(2)'}(\gamma r_1)\} + \gamma^2 l d^2/2a\chi]}{4\mathrm{i}l/\{\pi r_1(\alpha-\beta)[H_n^{(2)'}(\gamma r_1)]^2\} + \gamma^2 l d^2/2a\chi}, \tag{4.12}$$

where the function χ, which was defined in (2.5), accounts for the influence of the vortex shedding. On comparing this expression with that given for the reflection coefficient of a plane backed liner, given in (2.12) and (2.13), we see that we have only introduced two new non-dimensional parameters: the Helmholtz number γr_1 of the liner radius, and the azimuthal variation parameter n. As we have already mentioned, the radial component γ of the wavenumber k_0 plays the same role for the cylindrical liner as the normal component $k_0 \cos\theta$ does for the plane liner. Therefore the resonance parameter Q which we defined in §2 for a plane liner appears in this expression;

$$Q = \gamma^2 l d^2/2a. \tag{4.13}$$

For the plane liner, we saw that when the cavity is acoustically compact this resonance parameter is nearly unity at the position of peak absorption coefficient when the frequency or mean flow is varied.

We can now examine the influence of curvature on the absorptive properties of a perforated lining in a duct by choosing a surface perforation geometry and bias-flow Strouhal number, then comparing the absorption coefficient of the cylindrical liner with that of a plane liner as the radius of the cylinder is varied. For a plane backed screen, we showed in figure 3 that when the cavity-depth Helmholtz number is 0.5, total sound absorption occurs near $Q = 1$, $\kappa a = 2$. In figure 14, the dependence of the absorption coefficient $\Delta = 1 - |R|^2$ upon the Helmholtz number γr_1 of the liner radius is illustrated.

When there is no azimuthal variation ($n = 0$), the absorption coefficient does not fall below unity until the Helmholtz number γr_1 is very small. Consequently, when $n = 0$, a highly absorptive screech liner could be designed by assuming the liner to be a plane since in a jet pipe the radius of the liner greatly exceeds the cavity depth. However, as the azimuthal variation increases, so does the scale of the cylinder for which the liner may be assumed to be effectively plane.

There is some practical evidence to suggest that the azimuthal variation associated with screech is small. Therefore, our results show that a highly sound-absorbent screech liner could probably be designed by assuming the liner to be plane. In the next section, we examine how a source of sound radiates within a lined cylinder, in order to gain more insight into the effect of a liner on the sound field within the cylinder.

4.1. *The radiation from a source within a lined cylinder*

We have seen that perforated plates can offer large absorption at a particular frequency when a suitable combination of perforation geometry and bias-flow Strouhal number is chosen. Screech liners are usually designed by matching the Helmholtz resonance frequency of the liner to the expected screech frequency. The screech frequency is usually taken to be that associated with a resonance mode in an unlined rigid duct. However, when a liner is inserted, the boundary condition changes, and the resonance frequencies are altered. We can gain a useful idea of how the acoustical environment is altered when a liner is inserted by examining how a source radiates in this environment.

The sound field $G(\boldsymbol{r}\,|\,\boldsymbol{r}_0)$ produced by a point source at $\boldsymbol{r}_0$, and transmitted to an observation point $\boldsymbol{r}$, is described by the following inhomogeneous Helmholtz equation:

$$(\nabla^2 + k_0^2)\, G(\boldsymbol{r}\,|\,\boldsymbol{r}_0) = \delta(\boldsymbol{r} - \boldsymbol{r}_0). \tag{4.14}$$

The Fourier transform of this expression, according to the definition

$$\tilde{G}(r, n, k_z\,|\,\boldsymbol{r}_0) = \int_{-\infty}^{\infty} \int_{-\pi}^{\pi} G(\boldsymbol{r}\,|\,\boldsymbol{r}_0) \exp\left[-\mathrm{i}(k_z z + n\phi)\right] \mathrm{d}\phi\, \mathrm{d}z, \tag{4.15}$$

is then

$$\left[\frac{1}{r}\frac{\mathrm{d}}{\mathrm{d}r}\left(r\frac{\mathrm{d}}{\mathrm{d}r}\right) - \frac{n^2}{r^2} - k_z^2 + k_0^2\right] \tilde{G} = \frac{\delta(r - r_0)}{r_0} \exp\left[-\mathrm{i}(k_z z_0 + n\phi_0)\right]. \tag{4.16}$$

Since we require the solution to be finite on the cylinder axis,

$$\tilde{G} = A J_n(\gamma r) \quad \text{in} \quad 0 \leqslant r_0 \leqslant r, \tag{4.17}$$

where A is a constant. For the region between the source and the lined wall, we write

$$\tilde{G} = B[H_n^{(1)}(\gamma r) + R H_n^{(2)}(\gamma r)], \tag{4.18}$$

where B is a constant and R is the reflection coefficient of the lined cylinder which was given in (4.11).

The boundary conditions, from which we can determine the constants A and B, are obtained by integrating equation (4.16). We find that $\tilde{G}$ is continuous through the source at $r = r_0$ and the gradient of $\tilde{G}$ is discontinuous:

$$\left[\frac{\mathrm{d}\tilde{G}}{\mathrm{d}r}\right]_{r=r_0-0}^{r=r_0+0} = \exp\left[-\mathrm{i}(k_z z_0 + n\phi_0)\right]/r_0. \tag{4.19}$$

On applying these conditions to the solutions (4.17) and (4.18) we obtain the sound field $\tilde{G}$ due to the source at $r = r_0$:

$$\tilde{G} = \pi \Upsilon J_n(\gamma r_0) \exp\left[-\mathrm{i}(k_z z_0 + n\phi_0)\right]/2\mathrm{i}, \tag{4.20}$$

where

$$\Upsilon = [H_n^{(1)}(\gamma r) + R H_n^{(2)}(\gamma r)]/(1-R) \tag{4.21}$$

describes how a source radiates sound within the lined cylinder; the remaining terms in (4.20) depend solely on the structure of the source.

In terms of the surface impedance Z, whose relationship with the reflection coefficient is shown in (4.8), the radiation function Υ becomes

$$\Upsilon = \frac{\mathrm{i}\omega\rho_0[H_n^{(1)}(\gamma r_1) H_n^{(2)}(\gamma r) - H_n^{(1)}(\gamma r) H_n^{(2)}(\gamma r_1)] + \gamma Z[H_n^{(1)}(\gamma r) H_n^{(2)'}(\gamma r_1) - H_n^{(1)'}(\gamma r_1) H_n^{(2)}(\gamma r)]}{2[\gamma Z J_n'(\gamma r_1) - \mathrm{i}\omega\rho_0 J_n(\gamma r_1)]}. \tag{4.22}$$

On the wall of the liner at $r = r_1$ this function may be simplified. The first term in the numerator vanishes and the second is a function of the Wronskian which we encountered earlier, in (4.10). Thus

$$\Upsilon = \frac{-2\mathrm{i}Z/\pi r_1}{\gamma Z J_n'(\gamma r_1) - \mathrm{i}\omega\rho_0 J_n(\gamma r_1)} \quad \text{on} \quad r = r_1. \tag{4.23}$$

With the function Υ cast in this form we can see that when the magnitude of the surface impedance is large enough, the denominator is dominated by the first term. When $Z \to \infty$, the sound pressure on the surface of the lining is unbounded if the function $J_n'(\gamma r_1)$ vanishes. The surface impedance of a rigid liner with no apertures is infinite, and the modes of oscillation for which $J_n'(\gamma r_1)$ vanishes are then the resonance modes.

Screeching combustion is usually detected in engine tests by monitoring the sound pressure level near the wall of the jet pipe. The effect of a perforated liner on the surface sound pressure level can be assessed by plotting

$$S = 20 \log_{10} |[\Upsilon]_{r=r_1}| \tag{4.24}$$

against the Helmholtz number γr_1 of the liner radius. In particular, for a given radius r_1, the positions of peaks in this function correspond to wavenumbers at which a source can radiate more effectively causing large pressure fluctuations at the wall of the jet pipe; the absolute level of S is unimportant.

The non-dimensional parameters which we adopted in the previous section are: the resonance parameter Q, the Strouhal number κa, the cavity-depth Helmholtz number γl, the liner-radius Helmholtz number γr_1, and the azimuthal variation parameter n. We want to examine the sound field as a function of γr_1 for a particular liner, and so it is appropriate to replace Q, γl and κa by the following frequency-

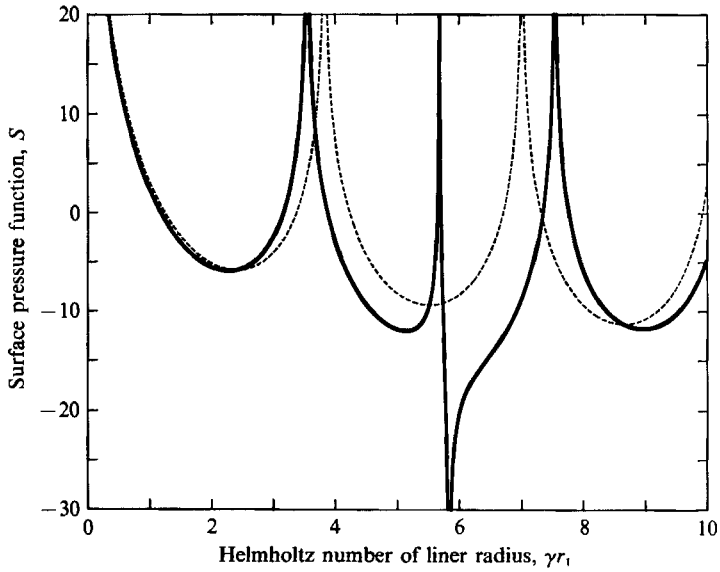

FIGURE 15. The variation of the function S when no absorption mechanism is present. Solid line, perforated lining; dashed line, unperforated (rigid) lining. $n = 0$, $l/r_1 = 0.05$, $a/l = 0.25$, $al/d^2 = 0.045$, $k_z/k_0 = 0$. The resonance parameter is equal to unity for the perforated liner at $\gamma r_1 = 6$.

independent parameters: the Mach number M, based on the mean velocity in the mouths of the apertures, the geometrical parameters l/r_1, a/l, and al/d^2, and the wavenumber ratio k_z/k_0. These two sets of non-dimensional parameters have the interrelation

$$\kappa a = \frac{\gamma r_1 (a/l)\,(l/r_1)}{M[1-(k_z/k_0)^2]^{\frac{1}{2}}},$$
$$\gamma l = \gamma r_1 (l/r_1),$$
$$Q = \frac{(\gamma r_1)^2\,(l/r_1)^2}{2al/d^2}.$$

In figure 15, the form of S is illustrated for a perforated liner with a resonance near $\gamma r_1 = 6$ when no sound absorption mechanism is included; that is, when the Rayleigh conductivity of the aperture is real and equal to twice the aperture radius. The dashed line in the figure shows the form of S when the liner is unperforated. Perforating the liner shifts the positions of the peaks and introduces a new peak because the liner itself has a resonant response. Using a perforated lining which offers little damping could therefore produce an engine which is more prone to screech. If there is no variation in the sound field along the duct, $k_z/k_0 = 0$, and therefore $\gamma \equiv k_0$. Typically, for an engine, $r_1 \approx 0.4$ m and $c \approx 440$ m/s, near the liner. Therefore the range of γr_1 plotted corresponds to a frequency range of up to about 1.8 kHz; a typical screech frequency is around 1.3 kHz. For this liner, the plane backed screen theory in §2 suggests that we should have $\kappa a = 3.4$ for high absorption at resonance. Therefore, since $k_z/k_0 = 0$, the Mach number of the bias flow should be approximately 0.022 for large absorption near $\gamma r_1 = 6$. The effect of such a mean flow is shown in figure 16. The peaks in the spectrum are now finite, and the height of the peak near $\gamma r_1 = 6$ is much reduced.

By altering the surface geometry and the mean bias flow velocity we can adjust the Helmholtz number γr_1 at which the peak absorption occurs. The absorption

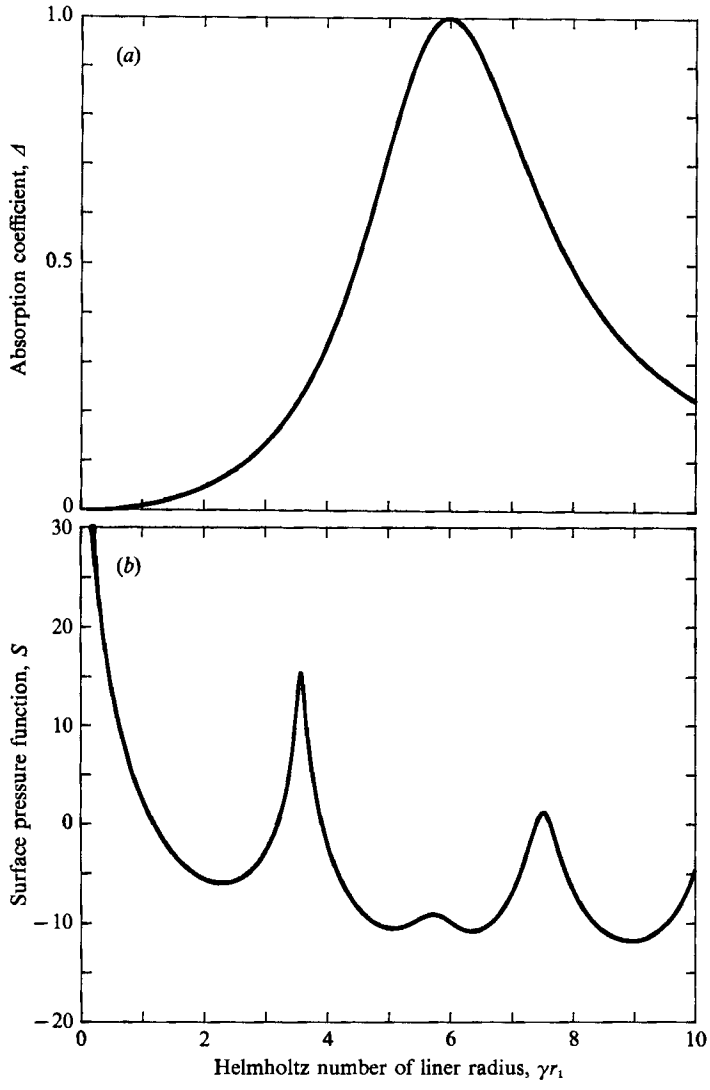

FIGURE 16. (*a*) The absorption coefficient, and (*b*) the function S, for a lined cylinder when sound is absorbed by vortex shedding. The source of sound and the geometry of the perforated liner are the same as that in figure 15 with $M = 0.022$.

coefficient curves for a plane liner can be used to choose the appropriate mean velocity for large absorption. In figures 17 and 18 we show how the function S is affected when the peak absorption is designed to occur near $\gamma r_1 = 4$ and 8 respectively. We see that the absorption curve is broader in the latter plot; significant absorption occurs over a larger range of γr_1.

Figures 16–18 show that, when there is no azimuthal variation of the sound source, a range of γr_1 over which the sound pressure level is reasonably uniform could be produced in our lined cylinder. In figures 19–21 we illustrate the way in which the absorptive property of a liner and the surface pressure function S are affected by azimuthal variation in the sound field; $n = 1$, 2, and 3, respectively. The geometry and flow conditions are the same as those in figure 18. The dotted lines show the form of S when the liner is unperforated. The range γr_1 over which the sound pressure level

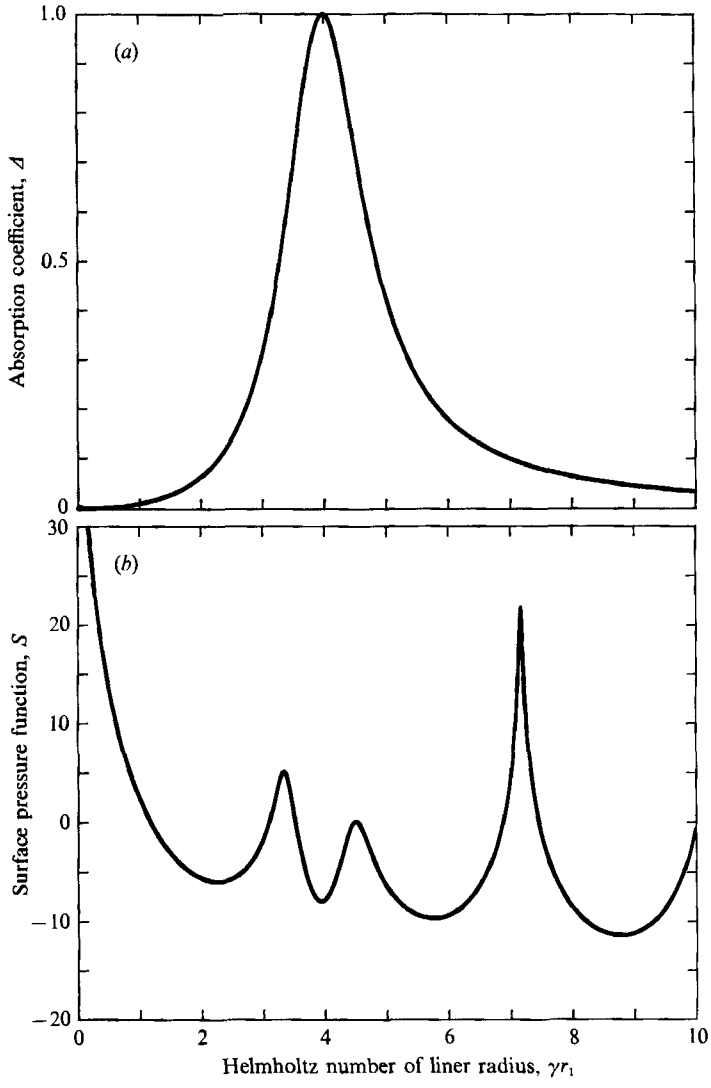

FIGURE 17. The effect of varying the resonance frequency of a perforated liner by altering the surface geometry and bias flow; $al/d^2 = 0.02, M = 0.01$. The resonance parameter is equal to unity at $\gamma r_1 = 4$. The source of sound is the same as in figure 16.

does not have large peaks is shifted to higher values of γr_1. However, as we have already mentioned, rapid azimuthal variation is unlikely in practice.

We conclude that a scheme for designing a liner where the effect of a particular liner on the sound field is examined may be more reliable than simply matching the Helmholtz resonance frequency to a screech frequency in an unlined duct.

4.2. *The effect of a velocity and temperature discontinuity*

In this section we present a simple extension to the preceding analysis with the aim of illustrating how the acoustic properties of a liner are likely to be affected by the mean flow of hot gas in the jet pipe. This axial mean flow is of finite, subsonic Mach number and is separated from the liner by a layer of cool air which is produced by blowing air through the perforations in the liner; we have already stressed the crucial

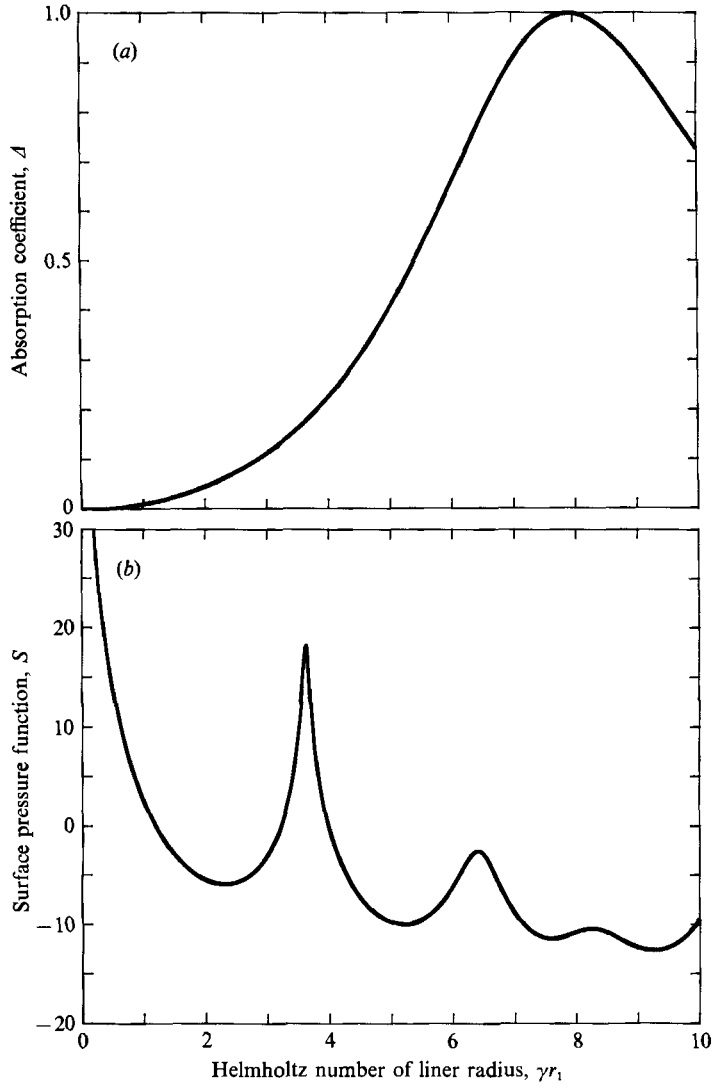

FIGURE 18. As figure 17 except for the surface geometry and bias flow; $al/d^2 = 0.08$, $M = 0.039$. The resonance parameter is equal to unity at $\gamma r_1 = 8$.

role of this bias flow. An idealized model of this situation is illustrated in figure 22. We assume that the thickness of the mixing region is small in comparison with the acoustic wavelength so that we can treat the variation in the axial velocity and temperature as a discontinuity. The mean velocity of the cool air is negligible except in the mouths of the apertures, where we assume that the flow is of the type that we have considered in the previous sections. The Rayleigh conductivity of the apertures which Howe (1979) determined then describes the scattering properties of the apertures if the presence of the velocity and temperature discontinuity can be ignored when describing the local aperture flow. Consequently, in the region beneath the discontinuity, the reflection coefficient of the cylindrical liner is assumed to be the same as that derived in (4.12).

This simple model should be appropriate provided that the thickness of the layer of cool air is large in comparison to the scale of the apertures; in practice, this is likely

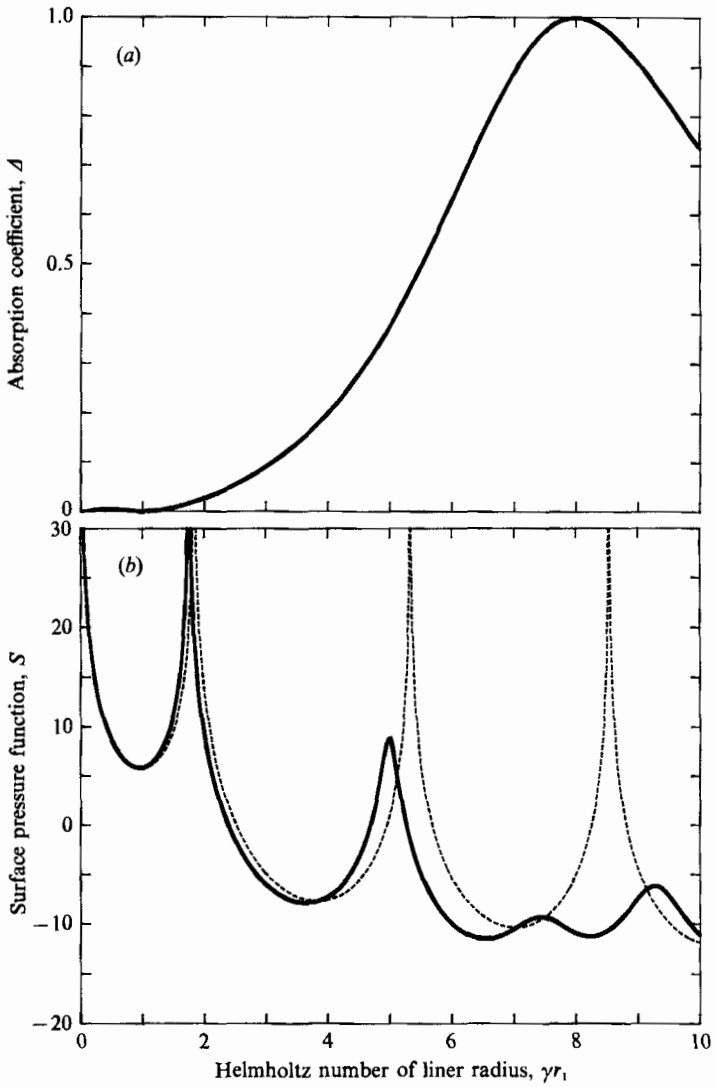

FIGURE 19. The effect of azimuthal variation in the sound field: $n = 1$. The geometry and bias flow are the same as in figure 18. The dashed line shows the form of the function S when the liner is unperforated.

to be true. The limit imposed on the validity of the model by this thickness arises because of the influence on the aperture flow of the vorticity which is shed from the aperture rims. If the layer of cool air is thin, then the interaction of the aperture wakes with the hot mean flow may be important. The scale on which to measure the thickness of the layer is the vorticity lengthscale $2\pi U/\omega = 2\pi a/\kappa a$, where U is the vorticity convection velocity and κa is the Strouhal number based on the aperture radius. When the Strouhal number is large, the sign of the vorticity changes over a small distance and so only the vorticity in the immediate vicinity of the aperture has a significant influence on the flow in the aperture. However, when the Strouhal number is small, vorticity of one sign is stretched over a large distance and vorticity many aperture diameters downstream can influence the aperture flow (Howe 1979). In the latter situation, one may expect the interaction between the aperture

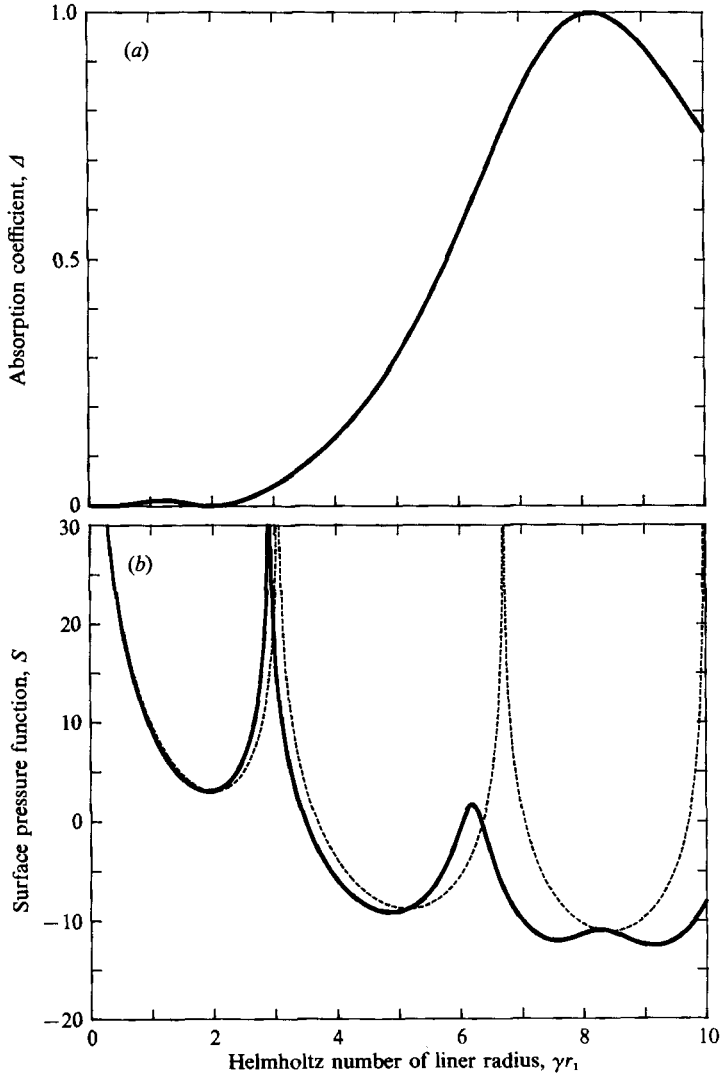

FIGURE 20. As figure 19 but for $n = 2$.

wakes and the velocity and temperature discontinuity to be important. When this is so, the model presented here may be of limited validity; although in support of our model we note that when the Strouhal number is small, the velocity of the flow through the apertures is large and the layer of cool air would be thicker than when the Strouhal number is large.

As in the previous sections, we shall represent the sound field in the duct as a linear combination of Hankel functions. The frequency measured in a frame which moves with the flow velocity U_v is ω_v. This is related to the frequency ω in a stationary frame through

$$\omega = \omega_v + k_z U_v \tag{4.25}$$

(Morse & Ingard 1968), where k_z is the axial wavenumber. If we define Θ as the angle between the normal to the wavefronts and the axial mean flow, then

$$k_z = k_v \cos\Theta, \tag{4.26}$$

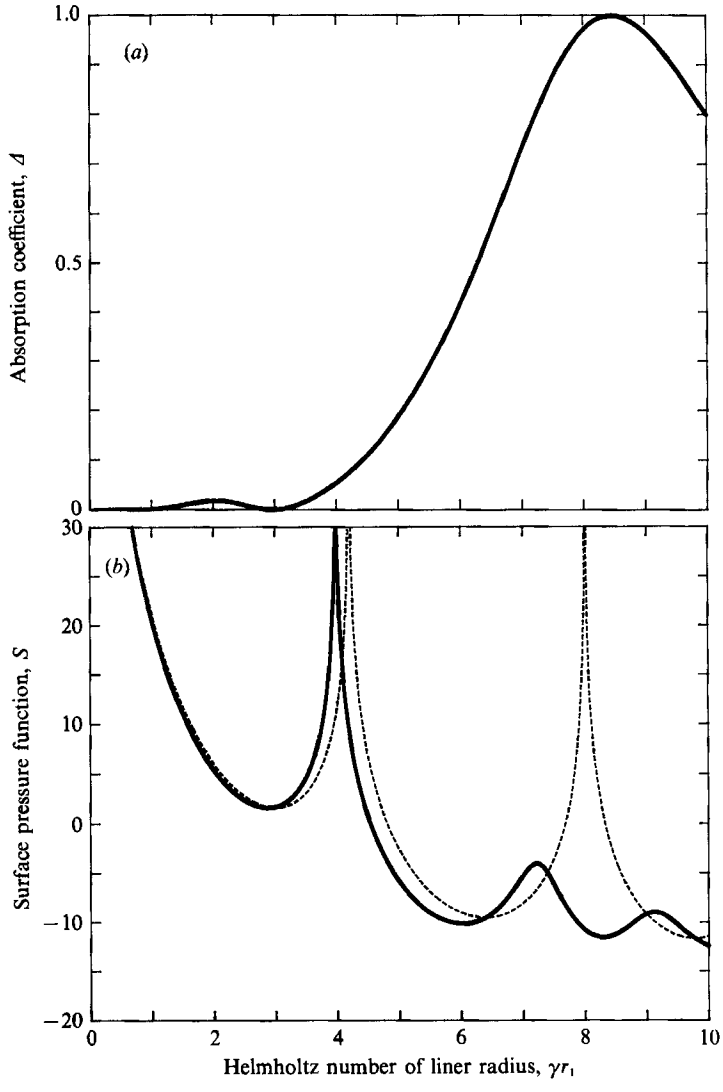

FIGURE 21. As figure 19 but for $n = 3$.

where $k_v = \omega_v/c_v$ and we obtain the familiar relationship

$$\omega = \omega_v(1+M_v\cos\Theta), \tag{4.27}$$

$M_v = U_v/c_v$ is the Mach number of the axial mean flow. The term $(1+M_v\cos\Theta)$ is commonly referred to as the Doppler factor.

In the region $r_0 < r < r_v$, exterior to a source region $r < r_0$, we write the sound pressure p as

$$p = H_n^{(1)}(\gamma_v r)+R_v H_n^{(2)}(\gamma_v r), \tag{4.28}$$

where

$$\gamma_v = \frac{\omega\sin\Theta}{c_v(1+M_v\cos\Theta)} \tag{4.29}$$

is the radial wavenumber. We have also introduced the reflection coefficient R_v of the whole region $r > r_v$ which we shall determine in terms of the properties of the fluid and the reflection coefficient of the liner. We shall then be able to examine how sound

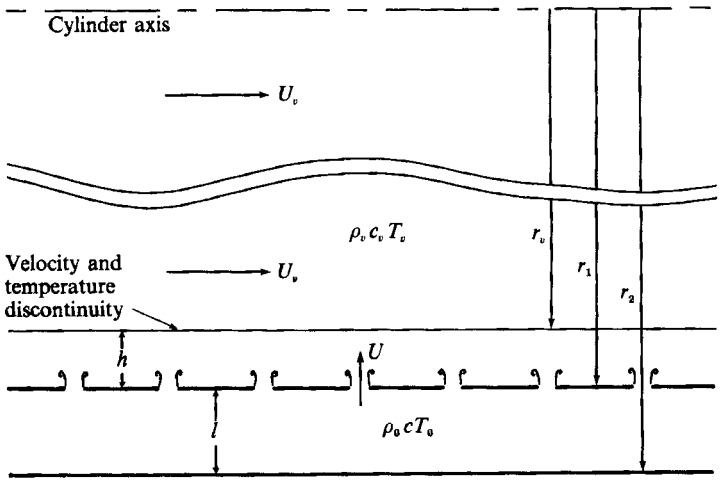

FIGURE 22. The geometry of the liner in the presence of a velocity and temperature discontinuity.

produced in the moving flow is absorbed by the combination of a cool layer and a perforated liner. The absorption coefficient A_v is the fraction of sound incident upon the surface $r = r_v$ that is absorbed. It is simply related to R_v through

$$A_v = 1 - |R_v|^2. \tag{4.30}$$

This expression is of the form considered in previous sections; the presence of the axial mean flow does not affect the form of the absorption coefficient even though sound energy is convected by the flow.

In the cool, stationary layer within $r_v < r < r_1$, the sound field is given by

$$p = A[H_n^{(1)}(\gamma r) + RH_n^{(2)}(\gamma r)], \tag{4.31}$$

where the radial wavenumber, γ, is equal to $(\omega^2/c^2 - k_z^2)^{\frac{1}{2}}$. When this relationship is combined with (4.26), we obtain

$$\gamma^2 = \omega^2/c^2 - \omega_v^2 \cos^2\Theta/c_v^2. \tag{4.32}$$

Equations (4.27) and (4.29) may be used to rearrange (4.32) to show that γ is related to γ_v by

$$\gamma = \frac{c_v \gamma_v}{c \sin\Theta}[(1 + M_v \cos\Theta)^2 - (c/c_v)^2 \cos^2\Theta]^{\frac{1}{2}}. \tag{4.33}$$

The reflection coefficient R_v is now determined by applying the appropriate boundary conditions for the velocity and temperature discontinuity: the sound pressure p and particle displacement ξ are both continuous across $r = r_v$. In $r < r_v$, the displacement ξ is related to the pressure gradient in the convected form of the linearized momentum equation

$$\frac{\partial p}{\partial r} = -\rho_v \left(\frac{\partial}{\partial t} + U_v \frac{\partial}{\partial z}\right)^2 \xi = -\rho_v(-\mathrm{i}\omega + \mathrm{i}k_z U_v)^2 \xi. \tag{4.34}$$

In the cool, stationary layer the equivalent relationship is simply

$$\frac{\partial p}{\partial r} = \rho_0 \omega^2 \xi. \tag{4.35}$$

On applying the boundary conditions, and using (4.26) and (4.27), we obtain

$$R_v = \frac{\left(\frac{\gamma\rho_v}{\gamma_v\rho_0}\right)\left[\frac{H_n^{(1)'}(\gamma r_v)+RH_n^{(2)'}(\gamma r_v)}{H_n^{(1)}(\gamma r_v)+RH_n^{(2)}(\gamma r_v)}\right]H_n^{(1)}(\gamma_v r_v)-H_n^{(1)'}(\gamma_v r_v)(1+M_v\cos\Theta)^2}{H_n^{(2)'}(\gamma_v r_v)(1+M_v\cos\Theta)^2-\left(\frac{\gamma\rho_v}{\gamma_v\rho_0}\right)\left[\frac{H_n^{(1)'}(\gamma r_v)+RH_n^{(2)'}(\gamma r_v)}{H_n^{(1)}(\gamma r_v)+RH_n^{(2)}(\gamma r_v)}\right]H_n^{(2)}(\gamma_v r_v)}. \tag{4.36}$$

This rather unwieldy expression simplifies in the limit of large Helmholtz number $\gamma_v r_v$. Some of the important features can then be examined more clearly. On replacing the Hankel functions and the reflection coefficient R by their asymptotic forms (see (4.9)) we obtain

$$R_v \sim \exp\left[2\mathrm{i}(\gamma_v r_v - \tfrac{1}{2}n\pi - \tfrac{1}{4}\pi)\right] \times \frac{\mathrm{i}(1+M_v\cos\Theta)^2[\gamma/\eta - 1/\tan\gamma l + \tan\gamma h] - \left(\frac{\gamma\rho_v}{\gamma_v\rho_0}\right)[\tan(\gamma h)(\gamma/\eta - 1/\tan\gamma l) - 1]}{\mathrm{i}(1+M_v\cos\Theta)^2[\gamma/\eta - 1/\tan\gamma l + \tan\gamma h] + \left(\frac{\gamma\rho_v}{\gamma_v\rho_0}\right)[\tan(\gamma h)(\gamma/\eta - 1/\tan\gamma l) - 1]}, \tag{4.37}$$

where $h = r_1 - r_v$ is the thickness of the cool layer above the screen, and η is the effective compliance of a plane perforated screen. For a screen with circular apertures this compliance was given in (2.4). As with the asymptotic form of the reflection coefficient for the cylindrical liner with a homogeneous, quiescent fluid inside the cylinder, the curvature of the liner does not affect the magnitude of R_v in this limit.

When η is real, no sound is absorbed by the screen, and we have the resonance condition

$$(1+M_v\cos\Theta)^2[\gamma/\eta - 1/\tan\gamma l + \tan\gamma h] = 0. \tag{4.38}$$

When this condition is satisfied, the reflection coefficient $|R_v| = 1$, and the surface at $r = r_v$ appears to be perfectly soft to sound waves incident upon it from $r < r_v$. We are not concerned with the relatively trivial solution $M_v\cos\Theta = -1$. The remaining expression reveals that it is only the thickness h of the cool layer above the liner which affects the condition for resonance; when the cool layer above the liner is vanishingly thin, the resonance condition of a plane liner in the absence of the temperature discontinuity is recovered. Intuitively, this result seems reasonable because the discontinuity reflects sound, and standing waves can therefore be set up in the region $r_v < r < r_1$ in much the same way as the standing waves in the cavity are set up, and it is the existence of standing waves which leads to the resonant behaviour.

The analogue Q_v of the resonance parameter Q which we used in the previous sections is then

$$Q_v = \gamma l(\gamma d^2/2a + \tan\gamma h) = Q + \gamma l\tan\gamma h, \tag{4.39}$$

when the cavity depth is sufficiently compact for $\tan\gamma l \approx \gamma l$. In practice it is likely that γh will be small, then $\tan\gamma h$ could also be replaced by its argument. We expect that when γr_1 is sufficiently large, then the peak absorption for given geometry and flow conditions should occur near $Q_v = 1$.

The presence of the discontinuity leads to the introduction of the following non-dimensional parameters: the impedance ratio $\rho_v c_v/\rho_0 c$, the Helmholtz number γh of the cool layer, the sound speed ratio c/c_v, the propagation direction Θ, and the component $M_v\cos\Theta$ of the Mach number in the propagation direction.

In figure 23 we illustrate the absorption coefficient Δ_v, as given by (4.30), (4.36),

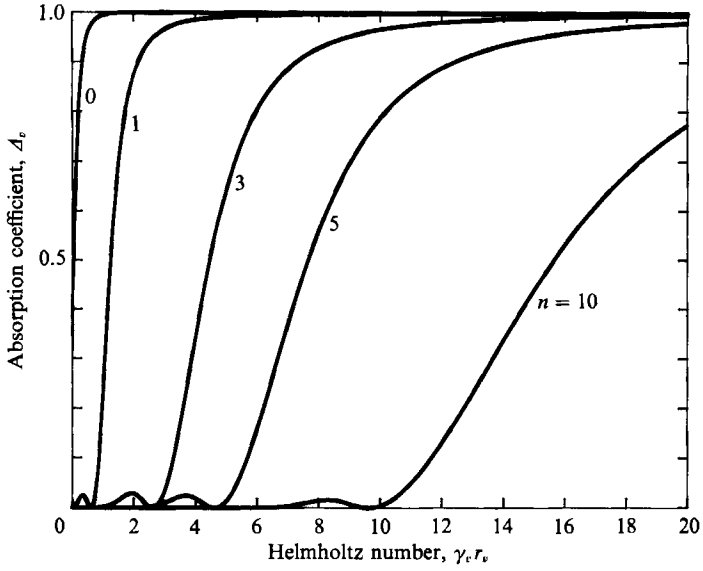

FIGURE 23. The absorption coefficient for a lined cylinder in the presence of a velocity and temperature discontinuity expressed as a function of the Helmholtz number $\gamma_v r_v$. $Q_v = 1$, $\kappa a = 3.2$, $\gamma l = 0.37$, $\gamma h = 0.2$, $\rho_v c_v/\rho_0 c = 0.8$, $\Theta = \frac{1}{2}\pi$. The curves are for sound fields with different azimuthal variation.

and (4.12), as a function of the Helmholtz number $\gamma_v r_v$ when the resonance parameter Q_v is set equal to unity. This figure has a similar form to figure 14, and shows that, for small azimuthal variation, the absorption coefficient rises quickly to the value predicted by assuming the liner to be planar, which in this case is unity. All the sound can still be absorbed when the temperature and velocity discontinuity is present. The simple procedure for designing an absorptive liner by assuming it to be planar and then examining the sound field inside the cylinder with the chosen liner should still be appropriate.

In figures 24(*a*) and 24(*b*), the absorption coefficient for an effectively plane liner is plotted as a function of the Strouhal number κa based on the mean velocity in the mouth of the apertures (which is approximately equal to the vorticity convection velocity). We have set the resonance parameter $Q_v = 1$, $\gamma l = 0.37$, $n = 0$ and $\Theta = \frac{1}{2}\pi$ (so that Doppler effects are excluded here). In figure 24(*a*), the impedance ratio $\rho_v c_v/\rho_0 c$ is varied and $\gamma h = 0.2$. In figure 24(*b*), the Helmholtz number of the cool layer is varied while $\rho_v c_v/\rho_0 c = 0.8$. The absorptive properties appear to be relatively insensitive to the thickness of the cool layer. This is rather fortunate because this length is arguably one of the more difficult parameters to estimate. Figures of this type could be used when choosing the geometry and bias flow for a particular liner when the discontinuity is significant, in much the same way as we used figure 4 to design a liner when the discontinuity was absent.

A similar procedure to that followed in §4.1 may now be used to examine the effect of the hot mean axial flow on the radiation from a source of sound in a lined duct. Referring to (4.21) we see that, on $r = r_v$, the function Υ which describes the environment into which the source radiates becomes

$$\Upsilon_v = \frac{H_n^{(1)}(\gamma_v r_v) + R_v H_n^{(2)}(\gamma_v r_v)}{1 - R_v}. \tag{4.40}$$

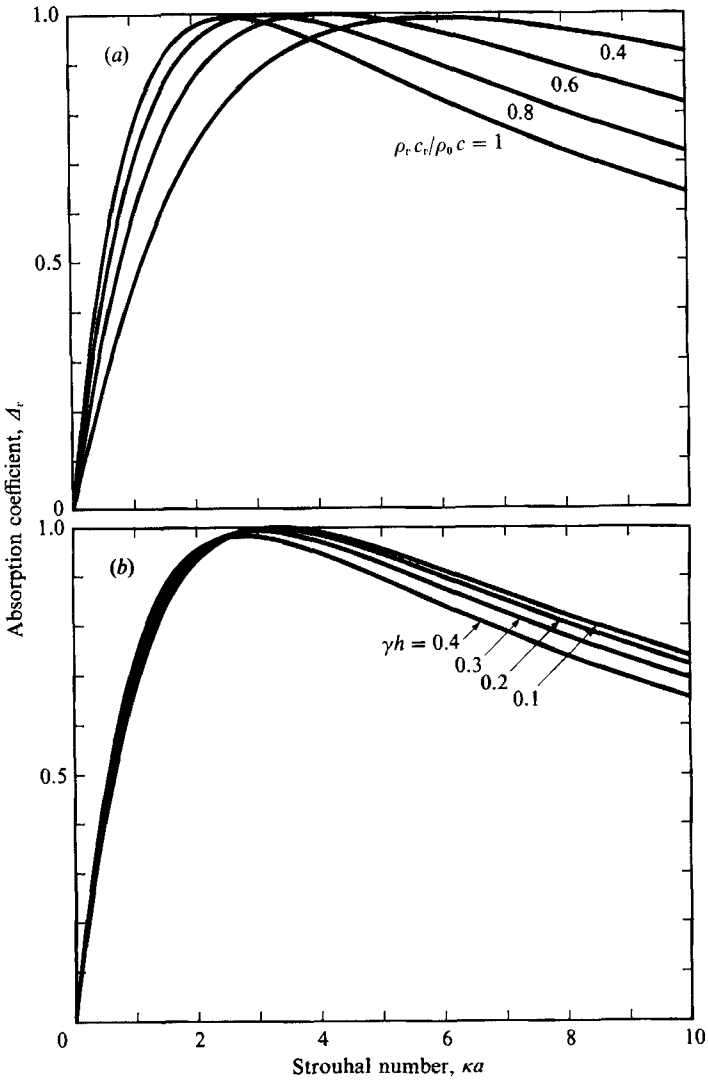

FIGURE 24. The absorption coefficient as a function of the Strouhal number κa for an effectively plane liner. $Q_v = 1$, $\gamma l = 0.37$, $n = 0$, $\Theta = \frac{1}{2}\pi$, $c/c_v = 0.62$. (*a*) $\gamma h = 0.2$, (*b*) $\rho_v c_v/\rho_0 c = 0.8$.

However, it is more sensible to examine the surface pressure on $r = r_1$, and there we find that the sound field $\tilde{G}$ is related to the source and surface properties through

$$\tilde{G} = \left[\frac{\pi J_n(\gamma r_0)\, \mathrm{e}^{-\mathrm{i}(n\phi_0 + k_z z_0)}}{2\mathrm{i}}\right]\left\{\frac{H_n^{(1)}(\gamma r_1) + RH_n^{(2)}(\gamma r_1)}{H_n^{(1)}(\gamma r_v) + RH_n^{(2)}(\gamma r_v)}\right\}\Upsilon_v, \tag{4.41}$$

where R is the reflection coefficient of the perforated liner in the absence of the discontinuity, and is given in (4.12). We introduce the function S_v which describes the sound pressure level on the surface produced by the source:

$$S_v = 20\log_{10}\left|\Upsilon_v\left\{\frac{H_n^{(1)}(\gamma r_1) + RH_n^{(2)}(\gamma r_1)}{H_n^{(1)}(\gamma r_v) + RH_n^{(2)}(\gamma r_v)}\right\}\right|. \tag{4.42}$$

We now examine this function for a set of parameters typical for a real engine. We

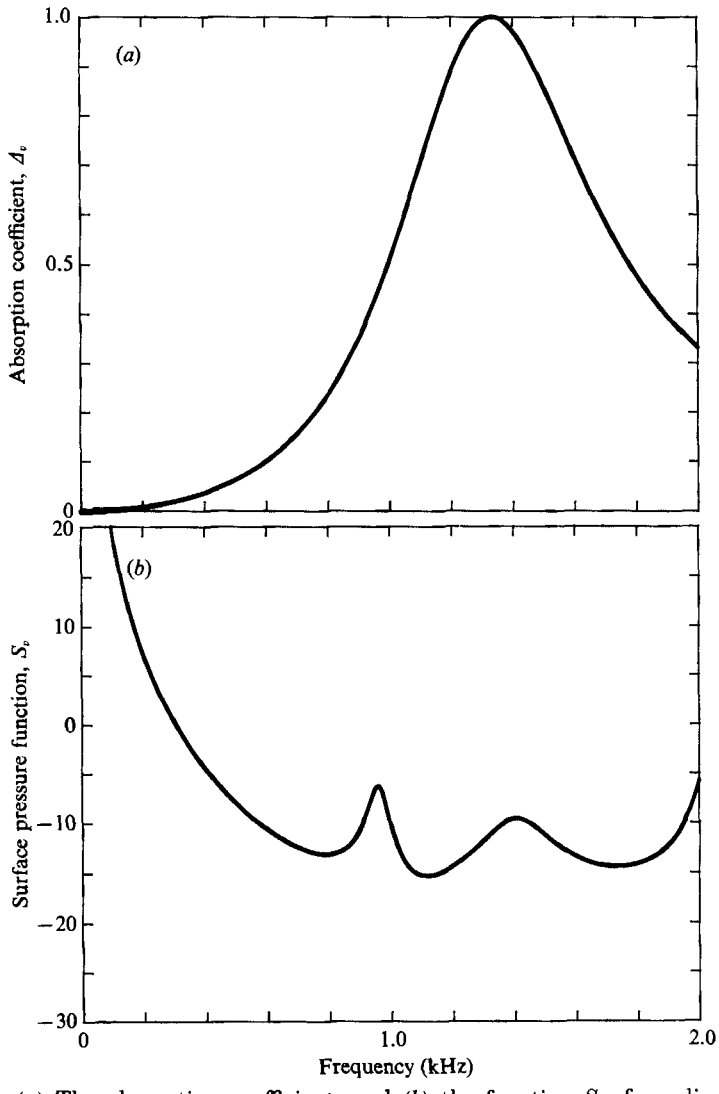

FIGURE 25. (*a*) The absorption coefficient, and (*b*) the function S_v, for a lined cylinder in the presence of a velocity and temperature discontinuity as a function of frequency. $a = 5$ mm, $l = 20$ mm, $d = 37$ mm, $U = 12.8$ m/s, $r_1 = 0.4$ m, $n = 0$, $\Theta = \frac{1}{2}\pi$, $h = 10$ mm, $T_v = 1300$ K, $T_0 = 500$ K, $\rho_0/\rho_v = 2$.

assume that the ratio of the specific heat capacities $c_p/c_v = 1.33$, and the gas constant $R = 287$ kJ/kgK, for both the hot and cool streams. We take $r_1 = 0.4$ m, $l = 0.02$ m, $T_v = 1300$ K, $T_0 = 500$ K, $h = 0.01$ m, $\rho_0/\rho_v = 2$ (therefore $\rho_v c_v/\rho_0 c = 0.8$). Also, for the purpose of choosing the geometry and flow through the liner so that all the sound around the frequency 1.3 kHz is absorbed, the liner is assumed to be plane, $n = 0$, and $\Theta = \frac{1}{2}\pi$. The resonance parameter $Q_v = 1$ when $a = 0.005$ m and $d = 0.037$ m. At 1.3 kHz, $\gamma l = 0.37$, so from figures 24(*a*) and 24(*b*) we see that $A_v \approx 1$ near $\kappa a = 3.2$. This implies that we should set the mean flow velocity in the mouths of the apertures equal to 12.8 m/s.

The absorption coefficient is plotted as a function of frequency in figure 25(*a*) when $n = 0$. The liner is then effectively plane over practically all the frequency range. The

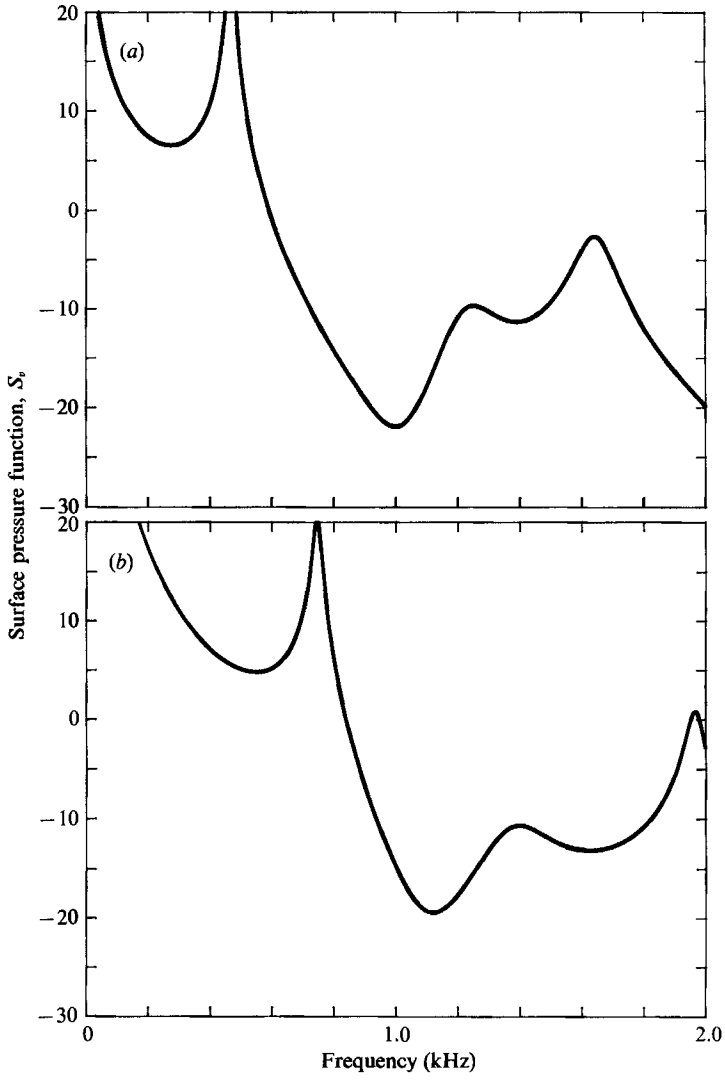

FIGURE 26. The effect of azimuthal variation in the sound field. The conditions are the same as in figure 25 except (*a*) $n = 1$, (*b*) $n = 2$.

corresponding form of the surface pressure function S_v, given in (4.42), is illustrated in figure 25(*b*). The peaks in the spectrum are relatively small and the liner thus appears to be quite effective. In figures 26 and 27(*a*) the effect of azimuthal variation in the sound field is illustrated. The liner then performs less well. However, as we have already noted, it is suspected that the azimuthal variation is small in practice. In the last of this set of figures, figure 27(*b*), $\Theta = 0.89\frac{1}{2}\pi$ rad. The mean axial flow then affects the results, and we have set $U_v = 140$ m/s ($M_v = 0.2$). Comparing this plot with figure 25(*b*), we see that perhaps the most striking feature is the difference between the curves above about 1.6 kHz; in figure 27(*b*) S_v decreases quite rapidly above this frequency. There is little or no experimental data available on the value of Θ, but it is usually assumed that the waves are normally incident; $\Theta = \frac{1}{2}\pi$.

In this section we have shown, by way of an elementary analysis, that the presence of a temperature and velocity discontinuity affects the criteria for designing a liner.

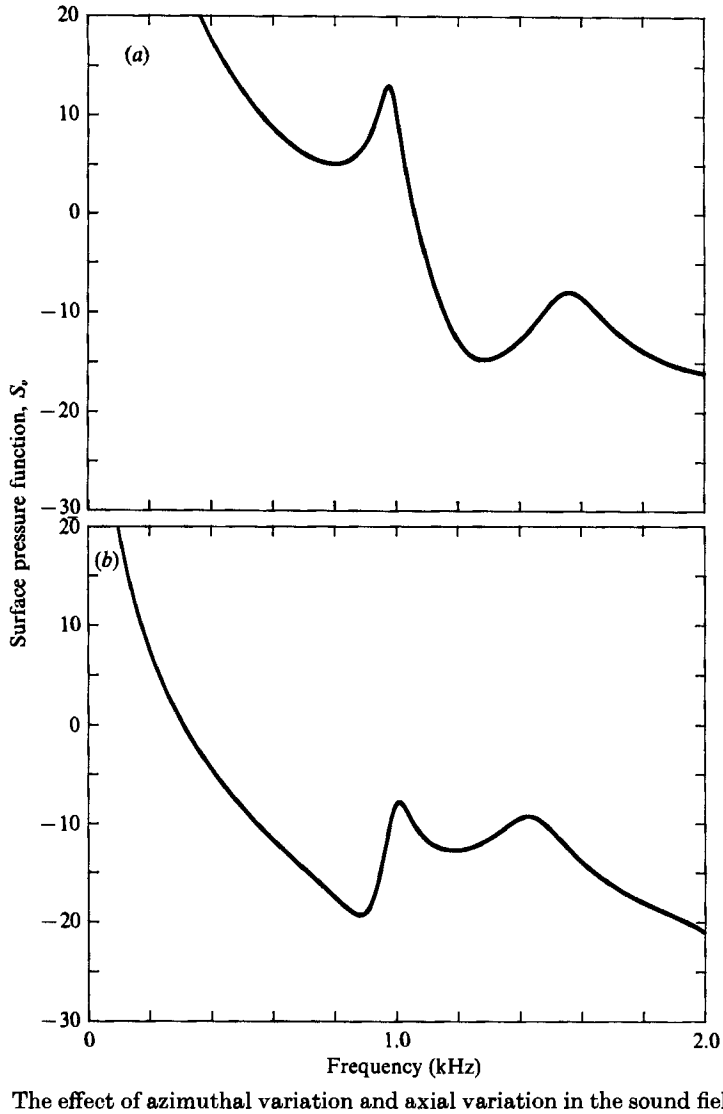

FIGURE 27. The effect of azimuthal variation and axial variation in the sound field. The conditions are the same as in figure 25 except that (*a*) $n = 3$, (*b*) $n = 0$, $\Theta = 0.89\frac{1}{2}\pi$, $M_v = 0.2$.

A highly absorptive liner may still be designed. We conclude that the peaks in the pressure near the wall of an unlined duct may be greatly reduced by such a liner over a useful frequency range. In theory a liner may be designed so that, over a range of frequencies at which a reheat flame is thought to be susceptible to screech, the sound pressure near the surface remains acceptably close to the background noise level.

5. Conclusions

We have shown that perforated liners with a bias flow through the apertures can absorb sound very effectively. At a particular frequency all the incident sound may be absorbed. If properly designed, such liners may suppress over a useful frequency range the peaks in the sound pressure spectrum which occur in those jet engines that use afterburners. The mean bias flow of cooling air through these liners plays a

crucial role in the absorption mechanism; the maximum absorption which a particular liner can offer is determined by the Strouhal number based on the aperture dimension.

We first examined the absorptive properties of plane liners with circular apertures. Experimental results have been presented which show encouraging agreement with our theoretical model. A screech liner is cylindrical. We have investigated the effects of curvature on the absorptive properties of a liner and shown that a highly absorptive liner can be designed by assuming that it is planar provided that the azimuthal variation in the sound field is small. The radiation from a source of sound within a lined cylinder is modified by the surface properties and so the frequencies at which an engine may screech are likely to be altered. We have examined the surface pressure fluctuations produced by a source within a lined cylinder and the results give a useful insight into the effectiveness of a particular liner. Such an examination may well lead to a more appropriate liner design than the usual procedure whereby the Helmholtz resonance frequency of a liner is simply matched to the frequency at which screech occurs in an unlined engine.

The hot, axial jet flow affects the acoustic properties of a liner: the frequency at which maximum sound absorption occurs is a function of the properties of both the hot gas and the cooling air. In §4.2 we presented a simple extension to the preceding theory and gave modified criteria for designing an effective liner.

The work described here was carried out while one author (I.J.H.) was in receipt of an SERC studentship. We should like to thank Mr Roy Carter who built the apparatus for the experimental work.

REFERENCES

ABRAMOWITZ, M. & STEGUN, I. A. 1965 *Handbook of Mathematical Functions*. Dover.

BARTHEL, F. 1958 Untersuchungen über nichtlineare Helmholtz-Resonatoren (Investigations on nonlinear Helmholtz resonators). *Frequenz* **12**, 1–11.

BECHERT, D. W. 1980 Sound absorption caused by vorticity shedding, demonstrated with a jet flow. *J. Sound Vib.* **70**, 389–405.

BLACKMAN, A. W. 1960 Effect of nonlinear losses on the design of absorbers for combustion in stabilities. *Am. Rocket Soc. J.*, November, 1022–1028.

BLOXSIDGE, G. J., DOWLING, A. P. & LANGHORNE, P. J. 1988 Reheat buzz: an acoustically coupled combustion instability. Part 2. Theory. *J. Fluid Mech.* **193**, 445–473.

BODEN, H. & ABOM, M. 1986 Influence of errors on the two-microphone method for measuring acoustic properties in ducts. *J. Acoust. Soc. Am.* **79**, 541–549.

CUMMINGS, A. 1983 Acoustic nonlinearities and power losses at orifices. *AIAA J.* **22**, 786–792.

CUMMINGS, A. 1984 Transient and multiple frequency sound transmission through perforated plates at high amplitude. *AIAA Paper* 84-2311.

DEAN, P. D. & TESTER, B. J. 1975 Duct wall impedance control as an advanced concept for acoustic suppression. *NASA CR*-134998.

GARRISON, G. D., SCHNELL, A. C., BALDWIN, C. D. & RUSSEL, P. R. 1969 Suppression of combustion oscillations with mechanical damping devices. *Interim Rep.* Pratt & Whitney Aircraft FR-3299.

HOWE, M. S. 1979 On the theory of unsteady high Reynolds number flow through a circular aperture. *Proc. R. Soc. Lond.* A **366**, 205–223.

INGARD, U. & LABATE, S. 1950 Acoustic circulation effects and the nonlinear impedance of orifices. *J. Acoust. Soc. Am.* **22**, 211–218.

LEPPINGTON, F. G. & LEVINE, H. 1973 Reflexion and transmission at a plane screen with periodically arranged circular or elliptical apertures. *J. Fluid Mech.* **61**, 109–127.

LEWIS, G. D. & GARRISON, G. D. 1971 The role of acoustic absorbers in preventing combustion instability. *AIAA Paper* 71-699.

MARKSTEIN, G. H. 1964 *Non-steady Flame Propagation*. Pergamon.

MELLING, T. H. 1973 The acoustic impedance of perforates at medium and high sound pressure levels. *J. Sound Vib.* **29**, 1–65.

MORSE, P. M. & INGARD, K. U. 1968 *Theoretical Acoustics*. McGraw-Hill.

RAYLEIGH, LORD 1899 On the theory of resonance. In *Scientific Papers*, Vol. I. Cambridge University Press.

RAYLEIGH, LORD 1945 *The Theory of Sound*, Vol. II. Dover. re-issue.

SEYBERT, A. F. & ROSS, D. F. 1977 Experimental determination of acoustic properties using a two-microphone random-excitation technique. *J. Acoust. Soc. Am.* **61**, 1362–1370.

SEYBERT, A. F. & SOENARKO, B. 1981 Error analysis of spectral estimates with application to the measurement of acoustic parameters using random sound fields in ducts. *J. Acoust. Soc. Am.* **69**, 1190–1199.

ZINN, B. T. 1970 A theoretical study of non-linear damping by Helmholtz resonators. *J. Sound Vib.* **13**, 347–356.